

## Appendix F Example Problems and Calculations

### F-1. General

This appendix presents a series of example problems and calculations. The examples illustrate the procedures used in the Simplified Bishop and Modified Swedish methods of slope stability analysis and provide guidance for checking and verifying the results of slope stability analyses. Examples for end-of-construction and steady seepage conditions are presented in this appendix. Examples for rapid drawdown are presented in Appendix G.

a. Manual and spreadsheet calculations of the type described here are performed to check the results of computer analyses of slope stability. These analyses are performed to check the factors of safety calculated for the critical slip surface, and for other slip surfaces considered significant. The slip surfaces used for these examples were selected to illustrate the computational procedures and are not the most critical slip surfaces for the slopes.

b. As discussed elsewhere in this manual, the soil mass above the slip surface is subdivided into vertical slices. Computer programs use more slices than are needed for hand calculations. Six to twelve slices are sufficient for hand calculations. Fewer than 6 slices do not provide sufficient accuracy, and more than 12 slices makes the computations unwieldy, especially for computations using graphical methods.

c. In the following examples, computations are performed beginning with the uppermost slice near the top of the slope and proceeding to the toe area, regardless of the direction that the slope faces. Thus, in some cases the computations are performed for slices from left-to-right and in other cases for slices from right-to-left, depending on the direction that the slope faces.

d. All of the computations for the procedures of slices were initially performed using a computer spreadsheet program and then summarized in tabular form. The spreadsheet calculations were performed with the number of significant figures used by the spreadsheet program, with no arithmetic rounding. Values were rounded as appropriate for the tables presented in this appendix. Accordingly, some of the values may differ slightly from what might be calculated by hand. For example the value shown for the term  $W \sin \alpha$  may not be exactly equal to the values that would be computed using the values of the slice weight ( $W$ ) and the slope of the base of the slice ( $\alpha$ ) shown in the tables. Any such discrepancies caused by rounding off are insignificant.

### F-2. Simplified Bishop Method

The Simplified Bishop Method is only applicable to analyses with circular slip surfaces. The computations shown here have been performed using computer spreadsheet software. Detailed steps are presented below for a total stress analysis of a slope with no water and for an effective stress analysis of a slope with water, internal seepage, and external water loads.

a. *Slope without seepage or external water loads – total stress analyses.* Computations for the Simplified Bishop Method for slopes, where the shear strength is expressed in terms of total stresses and where there are no external water loads, are illustrated in Figure F-1. As for all of the examples presented, slices are numbered beginning with the uppermost slice and proceeding toward the toe of the slope. Once a trial slip surface has been selected, and the soil mass is subdivided into slices, the following steps are used to compute a factor of safety:

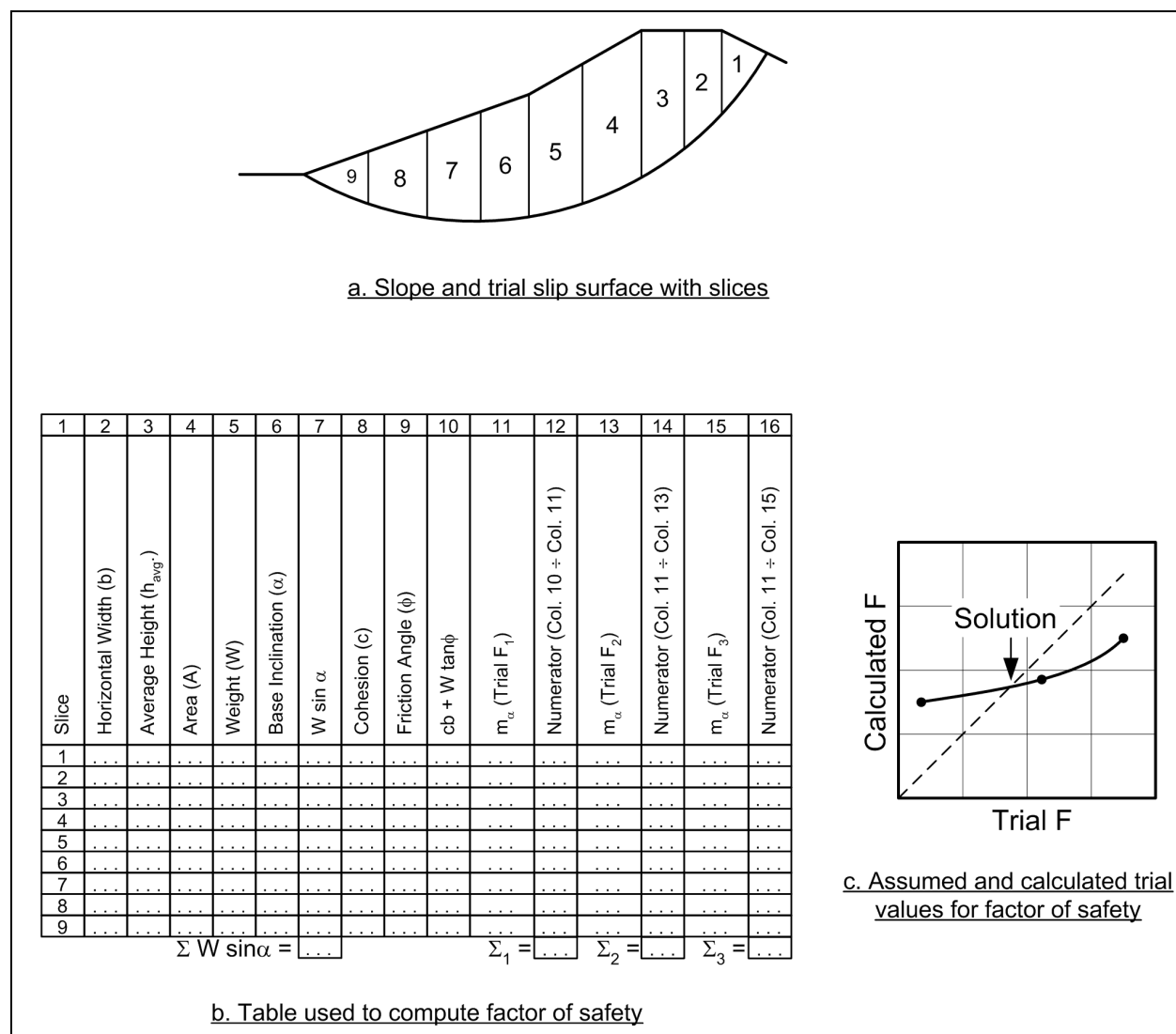


**Figure F-1. Simplified Bishop Method with no water - total stress analyses**

(1) The width,  $b$ , average height,  $h_{avg}$ , and inclination,  $\alpha$ , of the bottom of each slice are determined (Columns 2, 3, and 6 in Figure F-1b). The sign convention used throughout this appendix for the inclination,  $\alpha$ , is illustrated in Figure F-2. The inclination is positive when the base of the slice is inclined in the same direction as the slope.

(2) The area,  $A$ , of each slice is calculated by multiplying the width of the slice by the average height, i.e.,  $A = b h_{avg}$  (Column 4 in Figure F-1b).

(3) The weight of each slice is calculated by multiplying the total unit weight of soil by the area of the slice, i.e.,  $W = \gamma A$ . If the slice crosses zones having different unit weights, the slice is subdivided vertically into subareas, and the weights of the subareas are summed to compute the total slice weight (Column 5 in Figure F-1b).

(4) The quantity,  $W \sin \alpha$ , is computed for each slice, and these values are summed to obtain the term in the denominator of the equation for the factor of safety (Column 7 in Figure F-1b).

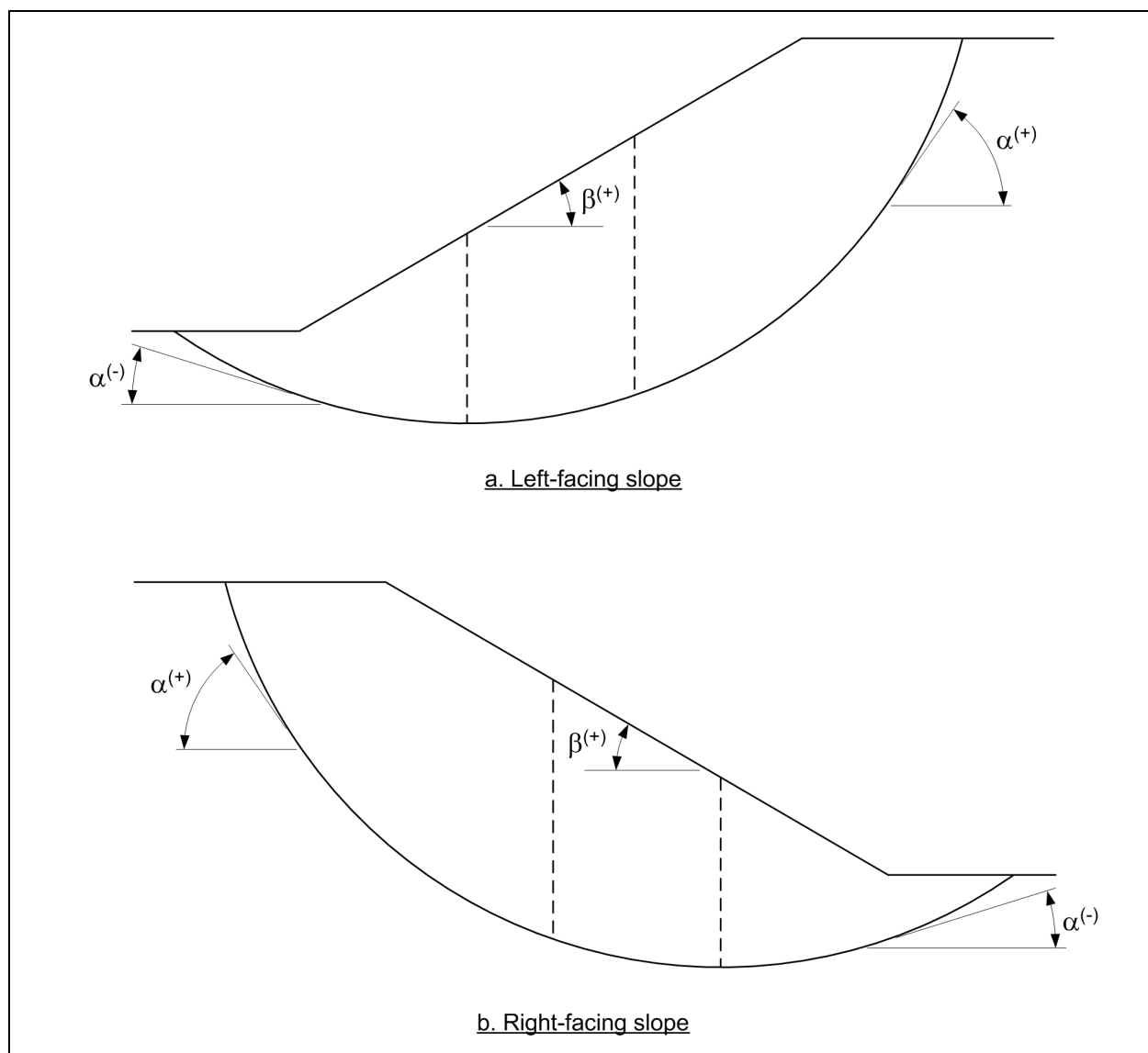


**Figure F-2. Sign convention used for angles  $\alpha$  and  $\beta$**

(5) The cohesion,  $c$ , and friction angle,  $\phi$ , for each slice are entered in Columns 8 and 9 in Figure F-1b. The shear strength parameters are those for the soil at the bottom of the slice; they do not depend on the soils in the upper portions of the slice.

(6) The quantity  $c \cdot b + W \tan(\phi)$  is computed for each slice (Column 10 in Figure F-1b).

(7) A trial value is assumed for the factor of safety and the quantity,  $m_\alpha$ , is computed from the equation shown below (Column 11 in Figure F-1b):

$$m_\alpha = \cos \alpha + \frac{\sin \alpha \tan \phi'}{F} \quad (F-1)$$

(8) The numerator in the expression for the factor of safety is computed by dividing the term  $cb + W \tan(\phi)$  by  $m_\alpha$  for each slice and then summing the values for all slices (Column 12 in Figure F-1b).

(9) A new factor of safety is computed from the equation:

$$F = \frac{\sum \left[ \frac{c \cdot b + W \cdot \tan \phi}{m_\alpha} \right]}{\sum W \sin \alpha} \quad (F-2)$$

This corresponds to dividing the summation of Column 12 by the summation of Column 7 in Figure F-1b.

(10) Additional trial values are assumed for the factor of safety and Steps 7 through 9 are repeated (Columns 13 through 16 in Figure F-1b). For each trial value assumed for the factor of safety, the assumed value and the value computed for the factor of safety using Equation F-2 are plotted as shown in Figure F-1c. The chart in Figure F-1c serves as a guide for selecting additional trial values. Values are assumed and new values are calculated until the assumed and calculated values for the factor of safety are essentially the same, i.e., until the assumed and calculated values fall close to the broken 45-degree line shown in Figure F-1c.

*b. Slope with seepage or external water loads – effective stress analyses.* Computations for slopes where the shear strength is expressed in terms of effective stresses, and where there are pore water pressures and external water loads, are illustrated in Figure F-3. In this case, the pore water pressures on the base of each slice must be determined. Loads from external water are included in all analyses, whether they are performed using total stress or effective stress. External water may be represented either as another soil, as described in Appendix C, or as an external force. In the description which follows, water is represented as an external load rather than as soil. Accordingly, a force on the top of the slice and the moment the force produces about the center of the circle must be computed. For a given trial circle, the following steps are required:

(1) For each slice the width,  $b$ , bottom inclination,  $\alpha$ , and average height,  $h_{avg}$ , are determined (Columns 2, 3, and 6 in Figure F-3c). The sign convention used for the angle,  $\alpha$ , is illustrated in Figure F-2.

(2) The area of the slice,  $A$ , is computed by multiplying the width of the slice by the average height,  $h_{avg}$ . (Column 4 in Figure F-3c).

(3) The weight,  $W$ , of the slice is computed by multiplying the area of the slice by the total unit weight of soil:  $W = \gamma A$  (Column 5 in Figure F-3c). If the slice crosses zones having different unit weights, the slice is subdivided vertically into subareas, and the weights of the subareas are summed to compute the total slice weight.

(4) The term  $W \sin \alpha$  is computed for each slice and then summed for all slices to compute  $\sum W \sin \alpha$  (Column 7 in Figure F-3c).

(5) The height,  $h_s$ , of water above the slice at the midpoint of the top of the slice is determined (Column 8 in Figure F-3c).

(6) The average water pressure on the top of the slice,  $p_{surface}$ , is calculated by multiplying the average height of water,  $h_s$ , by the unit weight of water (Column 9 in Figure F-3c).

(7) The inclination of the top of the slice,  $\beta$ , is determined (Column 10 in Figure F-3c). The sign convention for this angle is shown in Figure F-2.  $\beta$  is positive, except when the inclination of the top of the slice is opposite to the inclination of the slope. Negative values of  $\beta$  will exist when the inclination of the slope is reversed over some distance, such as a “bench” that is inclined inward toward the slope.

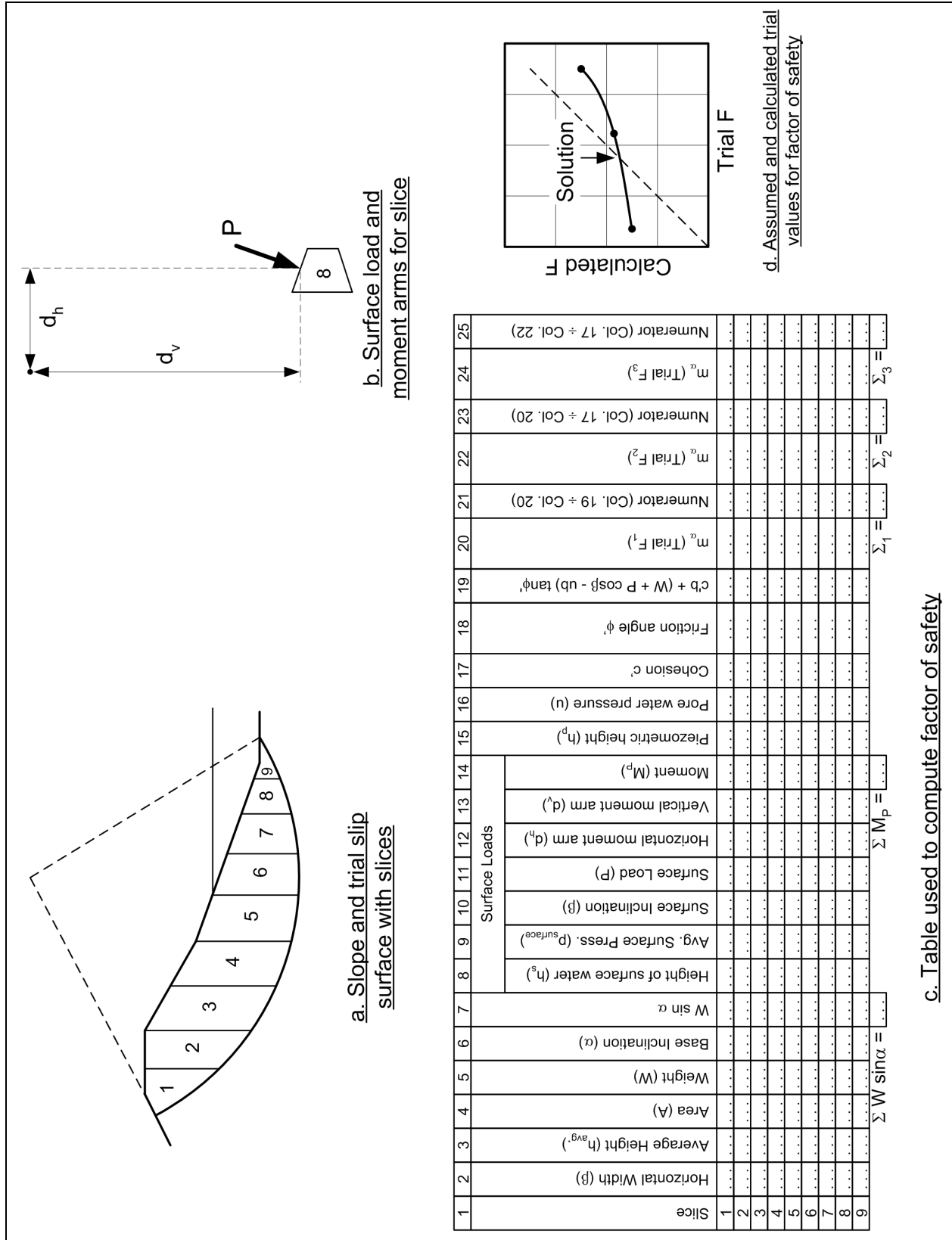


Figure F-3. Simplified Bishop Method with water - effective stress analyses

(8) The length of the top of the slice is multiplied by the average surface pressure,  $p_{\text{surface}}$ , to compute the external water force,  $P$ , on the top of the slice (Column 11 in Figure F-3c). The force  $P$  is equal to  $p_{\text{surface}} \cdot b / \cos(\beta)$ .

(9) The horizontal and vertical distances,  $d_h$  and  $d_v$ , respectively, between the center of the circle and the points on the top center of each slice are determined (Columns 12 and 13 in Figure F-3c). Positive values for these distances are illustrated in Figure F-3b. Loads acting at points located upslope of the center of the circle (to the left of the center in the case of the right-facing slope shown in Figure F-3) represent negative values for the distance,  $d_h$ .

(10) The moment,  $M_p$ , the result of external water loads is computed from the following (Column 14 in Figure F-3c):

$$M_p = P \cos \beta d_h + P \sin \beta d_v \quad (\text{F-3})$$

The moment is considered positive when it acts opposite to the direction of the driving moment produced by the weight of the slide mass, i.e., positive moments tend to make the slope more stable. Positive moments are clockwise for a right-facing slope like the one shown in Figure F-3.

(11) The piezometric height,  $h_p$ , at the center of the base of each slice is determined (Column 15 in Figure F-3c). The piezometric height represents the pressure head for pore water pressures on the base of the slice.

(12) The piezometric height is multiplied by the unit weight of water to compute the pore water pressure,  $u$  (Column 16 in Figure F-3c). For complex seepage conditions, or where a seepage analysis has been conducted using numerical methods, it may be more convenient to determine the pore water pressure directly, rather than evaluating the piezometric head and converting to pore pressure. In such cases Step 11 is omitted, and the pore water pressures are entered in Column 16.

(13) The cohesion,  $c'$ , and friction angle,  $\phi'$ , for each slice are entered in Columns 17 and 18 in Figure F-3c. The shear strength parameters are those for the soil at the bottom of the slice; they do not depend on the soils in the upper portions of the slice.

(14) The following quantity is computed for each slice (Column 19 in Figure F-3c):

$$c'b + (W + P \cos \beta - ub) \tan \phi' \quad (\text{F-4})$$

(15) A trial factor of safety,  $F_1$ , is assumed and the quantity,  $m_\alpha$ , is computed from the equation shown below (Column 20 in Figure F-3c):

$$m_\alpha = \cos \alpha + \frac{\tan \phi' \sin \alpha}{F_1} \quad (\text{F-5})$$

(16) The numerator in the equation used to compute the factor of safety is calculated by dividing the term  $c'b + (W + P \cos \beta - ub) \tan \phi'$  by  $m_\alpha$  for each slice and then summing the values for all slices (Column 21 in Figure F-3c).

(17) A new value is computed for the factor of safety using the following equation:

$$F = \frac{\sum \left[ \frac{c'b + (W + P \cos \beta - ub) \tan \phi'}{m_\alpha} \right]}{\sum W \sin \alpha - \frac{1}{R} \sum M_p} \quad (F-6)$$

where R is the radius of the circle.

The summations computed in Columns 7, 14, and 21 of the table in Figure F-3c are used to compute the new value for the factor of safety.

(18) Additional trial values are assumed for the factor of safety and steps 14 through 16 are repeated (Columns 22 through 25 in Figure F-3c). For each trial value assumed for the factor of safety, the assumed and calculated values of the factor of safety are plotted as shown in Figure F-3d, to provide a guide for selecting additional trial values. Values are assumed and new values are calculated until the assumed and calculated values for the factor of safety are essentially equal, i.e., until the assumed and calculated values fall close enough to the broken 45-degree line shown in Figure F-3d.

### F-3. Modified Swedish Method – Numerical Solution

The factor of safety can be calculated by the Modified Swedish Method using either numerical or graphical procedures. The numerical procedure is presented in this section and the graphical procedure is presented in Section F-4. Detailed steps are presented below for a total stress analysis of a slope with no water outside the slope and for an effective stress analysis of a slope with internal seepage and external water loads.

*a. Slope without seepage or external water loads – total stress analyses.* Computations for the Modified Swedish Method with total stresses and no external water loads are illustrated in Figure F-4. The Modified Swedish Method may be used with slip surfaces of any shape, and the procedure is the same regardless of the shape of the slip surface. For simplicity, a circle has been used for the example illustrated in Figure F-4. Once a trial slip surface has been selected and the soil mass has been subdivided into slices, the steps listed below are used to compute a factor of safety. Slices are numbered beginning with the uppermost slice and proceeding toward the toe of the slope.

(1) The width,  $b$ , average height,  $h_{avg}$ , and base inclination,  $\alpha$ , are determined (Columns 2, 3 and 6 in Figure F-4b).

(2) The area of the slice,  $A$ , is computed by multiplying the width,  $b$ , of the slice by the average height,  $h_{avg}$ . (Column 4 in Figure F-4b).

(3) The weight,  $W$ , of the slice is computed by multiplying the area of the slice by the total unit weight of soil:  $W = \gamma A$  (Column 5 in Figure F-4b). If the slice crosses zones having different unit weights, the slice is subdivided vertically into subareas, and the weights of the subareas are summed to compute the total slice weight.

(4) The length of the bottom of the slice,  $\Delta \ell$ , is determined; the length can be computed from the width,  $b$ , and base inclination,  $\alpha$ :  $\Delta \ell = b / \cos \alpha$  (Column 7 in Figure F-4b).

(5) The cohesion value,  $c$ , and friction angle,  $\phi$ , are determined for the base of each slice (Columns 8 and 9 in Figure F-4b). The shear strength parameters are those for the soil at the bottom of the slice; they do not depend on the soils in the upper portions of the slice.

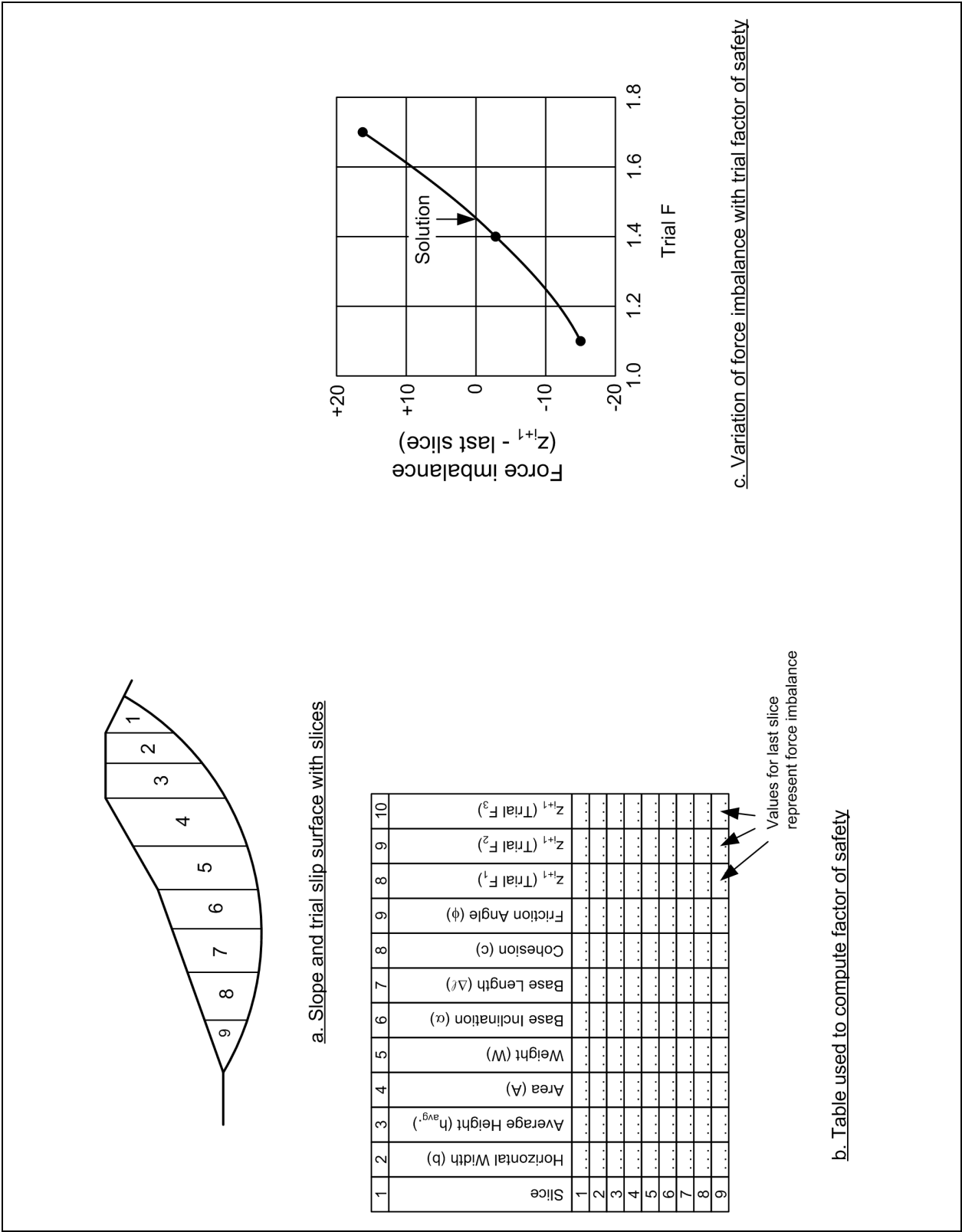


Figure F-4. Modified Swedish Method - numerical solution with no water - total stress analysis



(6) The inclination,  $\theta$ , of the interslice forces is determined. If the computations are being performed to check an analysis performed using Spencer's Method, the interslice force inclination determined from Spencer's Method should be used. Otherwise, the interslice force inclination should be assumed in accordance with the guidelines and discussion presented in Appendix C.

(7) A trial factor of safety,  $F_1$ , is assumed.

(8) Beginning with the first slice the side force,  $Z_{i+1}$ , on the "downslope" side (left side for the slope illustrated in Figure F-4) of each slice is computed from the equation:

$$Z_{i+1} = Z_i + \frac{W \left[ \sin \alpha - \frac{\tan \phi \cos \alpha}{F} \right] - \frac{c \cdot \Delta \ell}{F}}{\cos(\alpha - \theta) + \frac{\tan \phi \sin(\alpha - \theta)}{F}} \quad (F-7)$$

(9) If the force computed for the last slice,  $Z_{i+1}$ , is not sufficiently close to zero, a new trial value is assumed for the factor of safety and the process is repeated. By plotting the force imbalance,  $Z_{i+1}$ , for the last slice versus the factor of safety, the value of the factor of safety that satisfies equilibrium can usually be found to an acceptable degree of accuracy in about three trials (Figure F-4c).

*b. Slope with seepage or external water loads – effective stress analyses.* Computations for slopes where the shear strength is expressed in terms of effective stresses and where there are pore water pressures and external water loads are illustrated in Figure F-5. In addition to the quantities required when there is no water, the pore water pressures on the base of each slice, along with the forces from water on the top of the slice, must be determined. For a given trial slip surface, the following steps are required:

(1) For each slice, the width,  $b$ , average height,  $h_{avg}$ , and base inclination,  $\alpha$ , are determined (Columns 2, 3, and 6 in Figure F-5b).

(2) The area of the slice,  $A$ , is computed by multiplying the width,  $b$ , of the slice by the average height,  $h_{avg}$ . (Column 4 in Figure F-5b).

(3) The weight,  $W$ , of the slice is computed by multiplying the area of the slice by the total unit weight of soil:  $W = \gamma A$  (Column 5 in Figure F-5b). If the slice crosses zones having different unit weights, the slice is subdivided vertically into subareas, and the weights of the subareas are summed to compute the total slice weight.

(4) The piezometric height is determined at the upslope boundary, center and downslope boundary of each slice (Columns 7, 8, and 9 in Figure F-5b). The piezometric height at the upslope and downslope boundaries of the slice,  $h_i$  and  $h_{i+1}$ , respectively, are used to compute the forces from water pressures on the sides of the slice. Here, a triangular hydrostatic distribution of pressures is assumed on the sides of the slice. If the distribution of water pressures is more complex, it may be necessary to compute the water forces differently from what is illustrated in Figure F-5. Assuming triangular distributions of water pressures provides sufficient accuracy for most analyses. The piezometric height at the center of the slice,  $h_p$ , represents the pressure head for pore water pressures at the base of the slice (Column 8 in Figure F-5b).

(5) Hydrostatic forces from water pressures on the sides of the slice are computed from the equations shown below (Columns 10 and 11 in Figure F-5b):

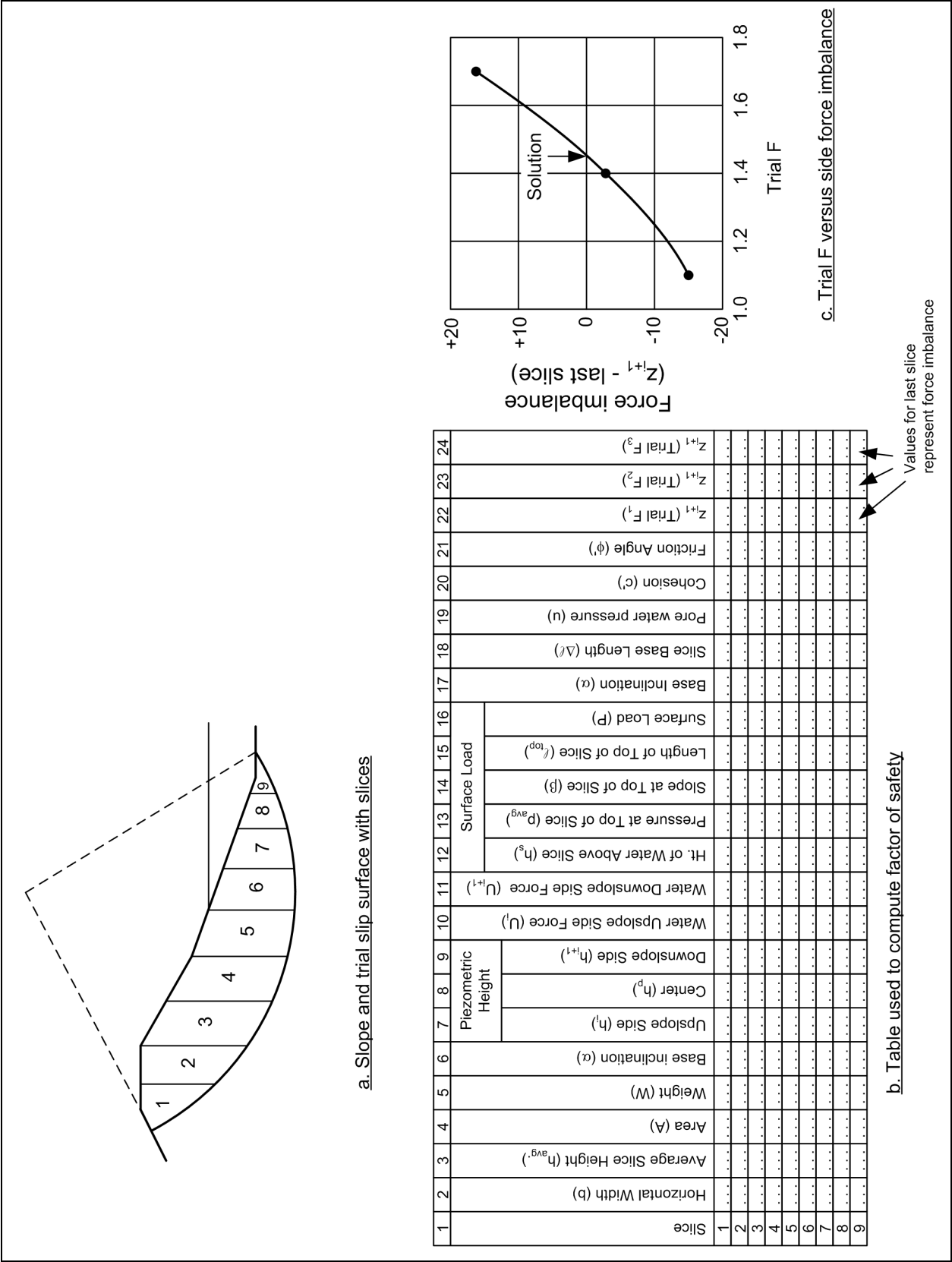


Figure F-5. Modified Swedish Method - numerical solution with water - effective stress analysis

$$U_i = \frac{1}{2} \gamma_w h_i^2 \quad (F-8)$$

and

$$U_{i+1} = \frac{1}{2} \gamma_w h_{i+1}^2 \quad (F-9)$$

where  $h_i$  and  $h_{i+1}$  are the heights determined in Step 4.

(6) The average height of water,  $h_s$ , above the top of the slice is determined (Column 12 in Figure F-5b). The height is used to compute the average water pressure and eventually the total force on the top of the slice (See Columns 13 and 16 in Figure F-5b). It is best to select the interslice boundaries so that a boundary is located at the point where the surface of the water outside the slope meets the slope. If this is done, the water pressures will vary linearly across each slice, and the average height of water is equal to the height of water above the midpoint of the slice.

(7) The average water pressure on the top of the slice,  $p_{avg}$ , is computed by multiplying the height of water,  $h_s$ , by the unit weight of water (Column 13 in Figure F-5b).

(8) The inclination of the top of the slice,  $\beta$ , is determined (Column 14 in Figure F-5b). This is the same as the inclination of the slope above the slice.

(9) The length of the top of the slice,  $\ell_{top}$ , is determined (Column 15 in Figure F-5b). The length can be computed from the relationship,  $\ell_{top} = b / \cos \beta$ .

(10) The water load on the top of the slice,  $P$ , is computed by multiplying the average water pressure,  $p_{avg}$ , by the length of the top of the slice,  $\ell_{top}$  (Column 16 in Figure F-5b).

(11) The length of the base of the slice,  $\Delta \ell$ , is computed from the relationship,  $\Delta \ell = b / \cos \alpha$  (Column 18 in Figure F-5b).

(12) The pore water pressure is computed by multiplying the piezometric head at the center of the base of the slice by the unit weight of water:  $u = \gamma_w h_p$  (Column 19 in Figure F-5b). For complex seepage conditions, or where a seepage analysis has been conducted using numerical methods, it may be more convenient to determine the pore water pressure directly, rather than evaluating the piezometric head and converting to pore pressure. In such cases, the pore water pressures are entered in Column 19.

(13) The cohesion and friction angle are determined for each slice depending on the soil at the bottom of the slice (Columns 20 and 21 in Figure F-5b). The shear strength parameters,  $c'$  and  $\phi'$ , are those for the soil at the bottom of the slice and do not depend on the soils located in the upper portions of the slice.

(14) The inclination,  $\theta$ , of the interslice forces is determined. If the computations are being performed to check an analysis performed using Spencer's Method, the interslice force inclination determined from Spencer's Method should be used. Otherwise, the interslice force inclination should be assumed in accordance with the guidelines and discussion presented in Appendix C.

(15) A trial value is assumed for the factor of safety, and interslice forces are calculated, slice-by-slice, to determine the force imbalance or "error of closure." The steps for this portion of the computations are the

same as those described for analyses with no water pressures, except the following equation for interslice forces is used:

$$Z_{i+1} = Z_i + \frac{W \left[ \sin \alpha - \frac{\tan \phi' \cos \alpha}{F} \right] + (U_i - U_{i+1}) \left[ \cos \alpha + \frac{\tan \phi' \sin \alpha}{F} \right] + P \left[ \sin (\alpha - \beta) - \frac{\tan \phi'}{F} \cos (\alpha - \beta) \right] - (c' - u \tan \phi') \frac{\Delta \ell}{F}}{\cos (\alpha - \theta) + \frac{\tan \phi' \sin (\alpha - \theta)}{F}} \quad (F-10)$$

(16) If the force computed for the last slice,  $Z_{i+1}$ , is not sufficiently close to zero, a new trial value is assumed for the factor of safety and the process is repeated. By plotting the force imbalance,  $Z_{i+1}$ , for the last slice versus the factor of safety, the value of the factor of safety that satisfies equilibrium can usually be found to an acceptable degree of accuracy in about three trials (Figure F-5c).

#### F-4. Modified Swedish Method – Graphical Solution

Graphical solution for the factor of safety by the Modified Swedish Method requires a trial and error process of assuming values for the factor of safety and constructing force equilibrium polygons until “closure” (force equilibrium) is established. Detailed steps are presented below for a total stress analysis of a slope with no water and for an effective stress analysis of a slope with water internal seepage and external water loads.

*a. Slope without seepage or external water loads – total stress analyses.* The graphical solution procedure using total stresses and no water pressures is illustrated in Figures F-6 and F-7. The calculations required to determine the magnitudes of the forces in the force polygons are shown in tabular form in Figure F-6; and the force polygons are shown in Figure F-7. The steps for determining the factor of safety once a trial shear surface is selected are as follows:

(1) For each slice the width,  $b$ , and the average height,  $h_{avg.}$ , are determined (Columns 2 and 3 in Figure F-6b).

(2) The area of the slice,  $A$ , is computed by multiplying the width,  $b$ , by the average height,  $h_{avg.}$ , of each slice (Column 4 in Figure F-6b).

(3) The slice weight,  $W$ , is computed by multiplying the area of the slice,  $A$ , by the total unit weight of soil,  $\gamma$ :  $W = \gamma A$  (Column 5 in Figure F-6b). If the slice crosses zones having different unit weights, the slice is subdivided vertically into subareas, and the weights of the subareas are summed to compute the total slice weight.

(4) The base length,  $\Delta \ell$ , for each slice is determined (Column 7 in Figure F-6). The base length may either be measured from a scaled drawing of the slope or computed by dividing the slice width,  $b$ , by the cosine of the inclination angle,  $\alpha$ , of the base of the slice, i.e.,  $\Delta \ell = b / \cos \alpha$ .

(5) The cohesion value,  $c$ , and friction angle,  $\phi$ , are determined for the base of each slice (Columns 8 and 9 in Figure F-6b). The shear strength parameters are those for the soil at the bottom of the slice; they do not depend on the soils in the upper portions of the slice.

(6) The available force resulting from cohesion is calculated by multiplying the cohesion value,  $c$ , by the length of the base of the slice,  $\Delta \ell$  (Column 10 in Figure F-6b).

(7) A trial value,  $F_1$ , is assumed for the factor of safety.

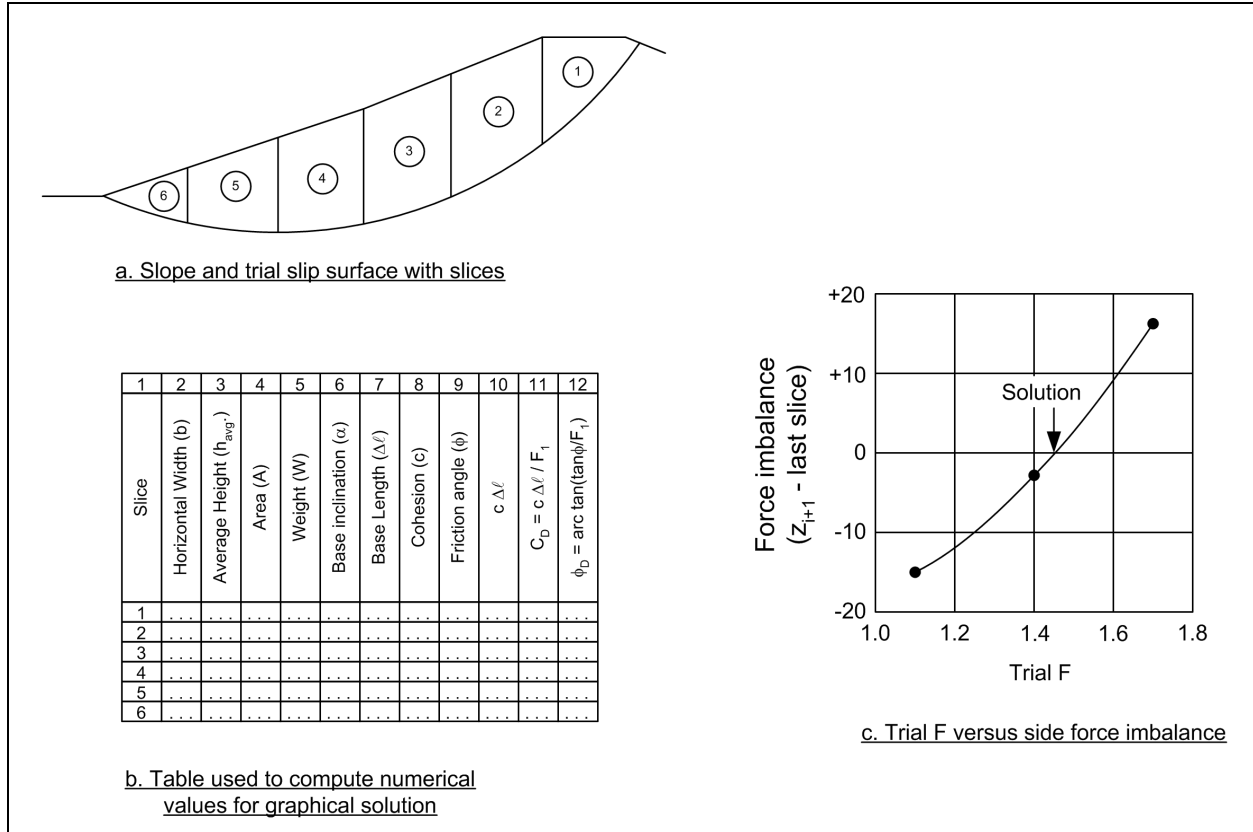


**Figure F-6. Modified Swedish Method - graphical solution with no water - slope and numerical table**

(8) The “developed” force from cohesion,  $C_D$ , is calculated by dividing the available force computed in Step 6 by the assumed value for the factor of safety:  $C_D = \frac{c \Delta \ell}{F_1}$  (Column 11 in Figure F-6b).

(9) The “developed” friction angle,  $\phi_D$ , is calculated from the relationship,  $\phi_D = \arctan\left(\frac{\tan \phi}{F_1}\right)$  (Column 12 in Figure F-6b).

(10) A suitable scale for force is selected and a vector representing the weight of the slice,  $W_1$ , is drawn vertically downward to start the equilibrium force polygons. The force polygons are illustrated in Figure F-7. Steps 11 through 17, which follow, are used to complete the forces in the force polygons, and to check for equilibrium. All vectors are drawn using the same force scale.

(11) A vector representing the developed cohesion force on the first slice,  $C_{D1}$ , is drawn in a direction parallel to the base of the first slice, extending from the tip of the weight vector drawn in Step 10.

(12) A line is drawn from the start (tail) of the weight vector in a direction perpendicular to the base of the slice. This line is shown as a broken line labeled  $N_1$  in Figure F-7b.

(13) A second line is drawn from the start (tail) of the weight vector so that the angle between the new line and line representing the normal vector ( $N_1$ ) is equal to the developed friction angle,  $\phi_D$ . The new line should be drawn such that the component of the vector parallel to the bottom of the slice acts in the direction of the resisting shear force, i.e., clockwise from the normal vector in the case of a left-facing slope. This

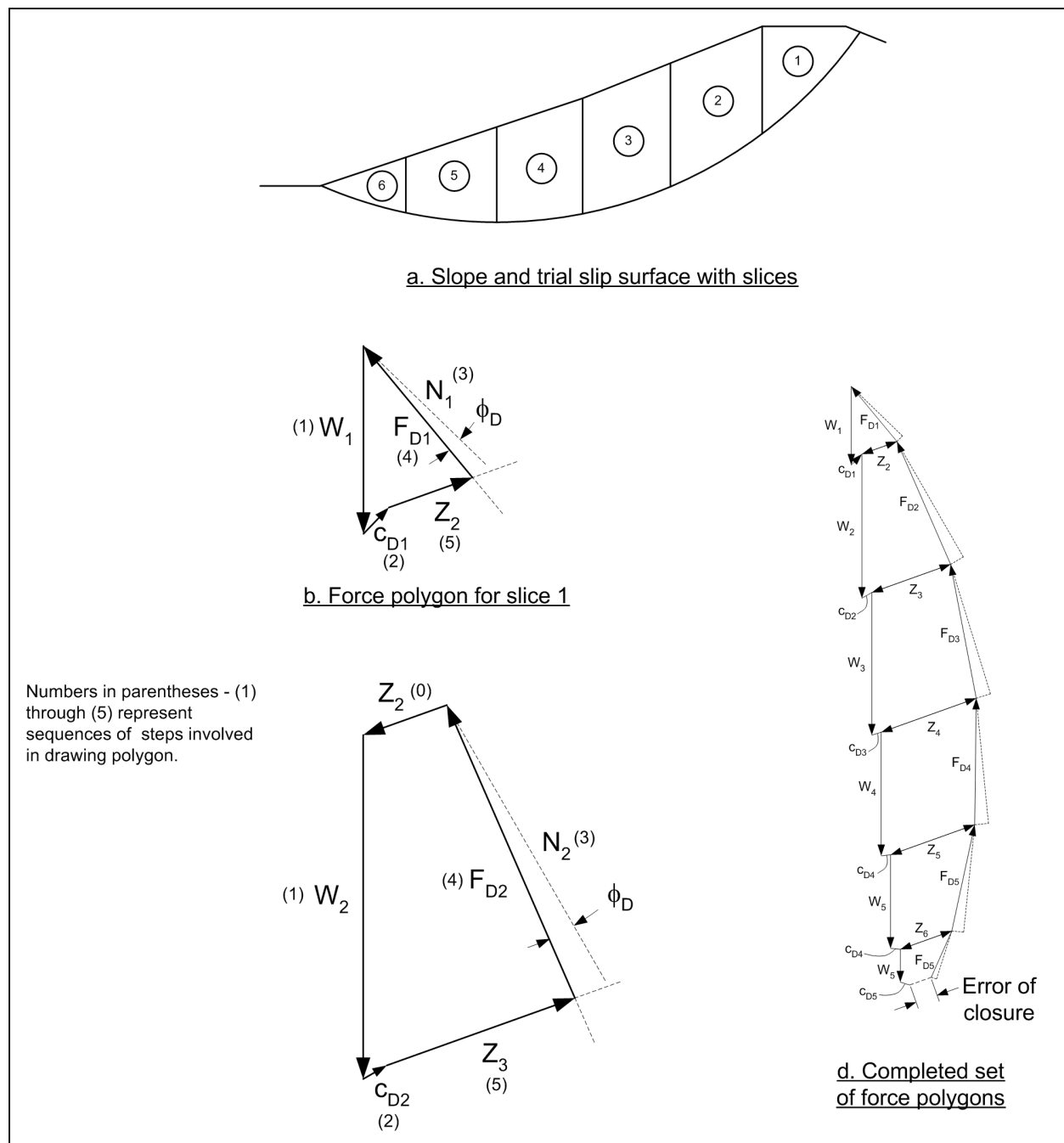


**Figure F-7. Modified Swedish method - graphical solution with no water - force polygons**

vector is labeled  $F_{D1}$  in Figure F-7b. If the soil at the bottom of the slice has  $\phi = 0$ , the lines drawn in Steps 11 and 12 are the same, i.e., the vectors  $N_1$  and  $F_{D1}$  are the same.

(14) A line is drawn from the tip (end) of the developed cohesion vector, in the direction assumed for the interslice forces. This line is labeled  $Z_2$  in Figure F-7b. If the computations are being performed to check computations that were performed using Spencer's Method, the interslice force inclination should be the one calculated in Spencer's Method. Otherwise, the interslice force inclination should be assumed in accordance with the guidelines and discussion presented in Appendix C.

(15) The intersection between the line directions drawn in Step 13 ( $F_D$ ) and Step 14 ( $Z_2$ ) is found. This defines the magnitudes of the forces  $F_{D1}$  and  $Z_2$ .

(16) The process continues by drawing the equilibrium force polygon for the next slice. A vector representing the weight of the slice is drawn vertically downward from the point where the cohesion and interslice force vectors,  $C_{D1}$  and  $Z_2$ , intersect. The force polygon for the second slice is shown in Figure F-7c. Closure of the force polygon is used to determine the magnitude of the forces  $F_{D2}$  and  $Z_3$  for the second slice.

(17) Force polygons are drawn consecutively, slice-by-slice, for all of the remaining slices. If the trial value of factor of safety is not the correct value, the force polygon for the last slice will not close. The error of closure is a measure of the inaccuracy in the assumed factor of safety. Additional trial values for the factor of safety are assumed until the force polygons close with an acceptable degree of accuracy. By plotting the error of closure versus the assumed values of factor of safety as shown in Figure F-6c, the correct value of factor of safety can usually be determined within a few trials.

*b. Slope with seepage or external water loads – effective stress analyses.* The graphical solution procedure for slopes where the shear strength is expressed in terms of effective stresses and where there are pore water pressures and external water loads are illustrated in Figures F-8 and F-9. The calculations required to determine the magnitudes of the forces in the force polygons are shown in tabular form in Figure F-8; and the force polygons are shown in Figure F-9. The steps for determining the factor of safety once a trial shear surface is selected are as follows:

(1) The width,  $b$ , average height,  $h_{avg}$ , and length of the slice base,  $\Delta\ell$ , are determined for each slice (Columns 2, 3, and 17 in Figure F-8b).

(2) The area of the slice is computed by multiplying the width,  $b$ , by the average height,  $h_{avg}$ . (Column 4 in Figure F-8b).

(3) The weight,  $W$ , of the slice is computed by multiplying the area by the total unit weight of soil:  $W = \gamma A$  (Column 5 in Figure F-8b). If the slice crosses zones having different unit weights, the slice is subdivided vertically into subareas, and the weights of the subareas are summed to compute the total slice weight.

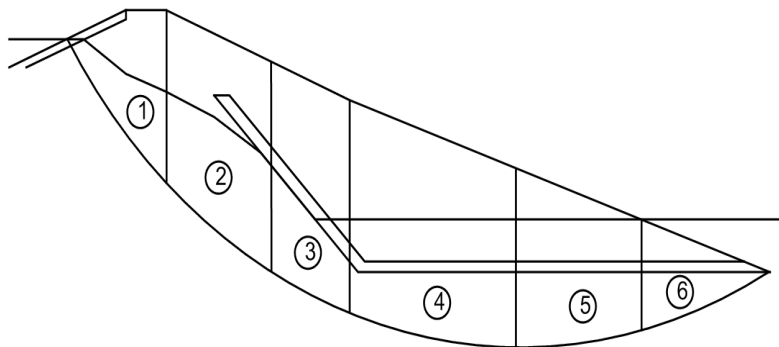
(4) The water loads on the sides and top of the slice are computed (Columns 7 through 16 in Figure 7b). The water loads are computed as described in Steps (4) through (10) in Section F-3b.

(5) The pore water pressure is computed by multiplying the piezometric head at the center of the base of the slice by the unit weight of water:  $u = \gamma_w h_p$  (Column 18 in Figure F-8b). For complex seepage conditions, or where a seepage analysis has been conducted using numerical methods, it may be more convenient to determine the pore water pressure directly, rather than evaluating the piezometric head and converting to pore pressure. In such cases the pore water pressures determined directly are entered in Column 18.

(6) The force,  $U_b$ , produced by the water pressure on the bottom of the slice is computed by multiplying the length of the base of the slice,  $\Delta\ell$ , by the pore water pressure,  $u$  (Column 19 in Figure F-8b).

(7) The “available” force resulting from cohesion is computed by multiplying the cohesion,  $c'$ , by the length of the base of the slice,  $\Delta\ell$ , (Column 22 in Figure F-8b).

(8) A trial value for the factor of safety,  $F$ , is assumed, and the developed cohesion force,  $C_D$ , is computed by dividing the available cohesion force by the factor of safety:  $C_D = c' \Delta\ell / F$  (Column 23 in



a. Slope and trial slip surface with slices

1	2	3	4	5	6	7	8	9	10	11	12	13	14	15	16	17	18	19	20	21	22	23	24
Slice	Horizontal Width (b)	Average Slice Height ( $h_{avg}$ )	Area (A)	Weight (W)	Base inclination ( $\alpha$ )	Piezometric Height			Water Upslope Side Force ( $U_i$ )	Water Downslope Side Force ( $U_{i+1}$ )	Ht. of Water Above Slice ( $h_s$ )	Pressure at Top of Slice ( $p_{avg}$ )	Slope at Top of Slice ( $\beta$ )	Length of Top of Slice ( $\ell_{top}$ )	Surface Load (P)	Slice Base Length ( $\Delta \ell$ )	Pore water pressure (u)	$U_b = u \Delta \ell$	Cohesion ( $c'$ )	Friction angle ( $\phi'$ )	$c' \Delta \ell$	$C_D = c' \Delta \ell / F$	$\phi_D = \arctan(\tan \phi' / F)$
1	...	...	...	...	...	...	...	...	...	...	...	...	...	...	...	...	...	...	...	...	...	...	...
2	...	...	...	...	...	...	...	...	...	...	...	...	...	...	...	...	...	...	...	...	...	...	...
3	...	...	...	...	...	...	...	...	...	...	...	...	...	...	...	...	...	...	...	...	...	...	...
4	...	...	...	...	...	...	...	...	...	...	...	...	...	...	...	...	...	...	...	...	...	...	...
5	...	...	...	...	...	...	...	...	...	...	...	...	...	...	...	...	...	...	...	...	...	...	...
6	...	...	...	...	...	...	...	...	...	...	...	...	...	...	...	...	...	...	...	...	...	...	...

b. Table used to compute numerical values for graphical solution

Figure F-8. Modified Swedish Method – graphical solution with water – slope and table of numerical values



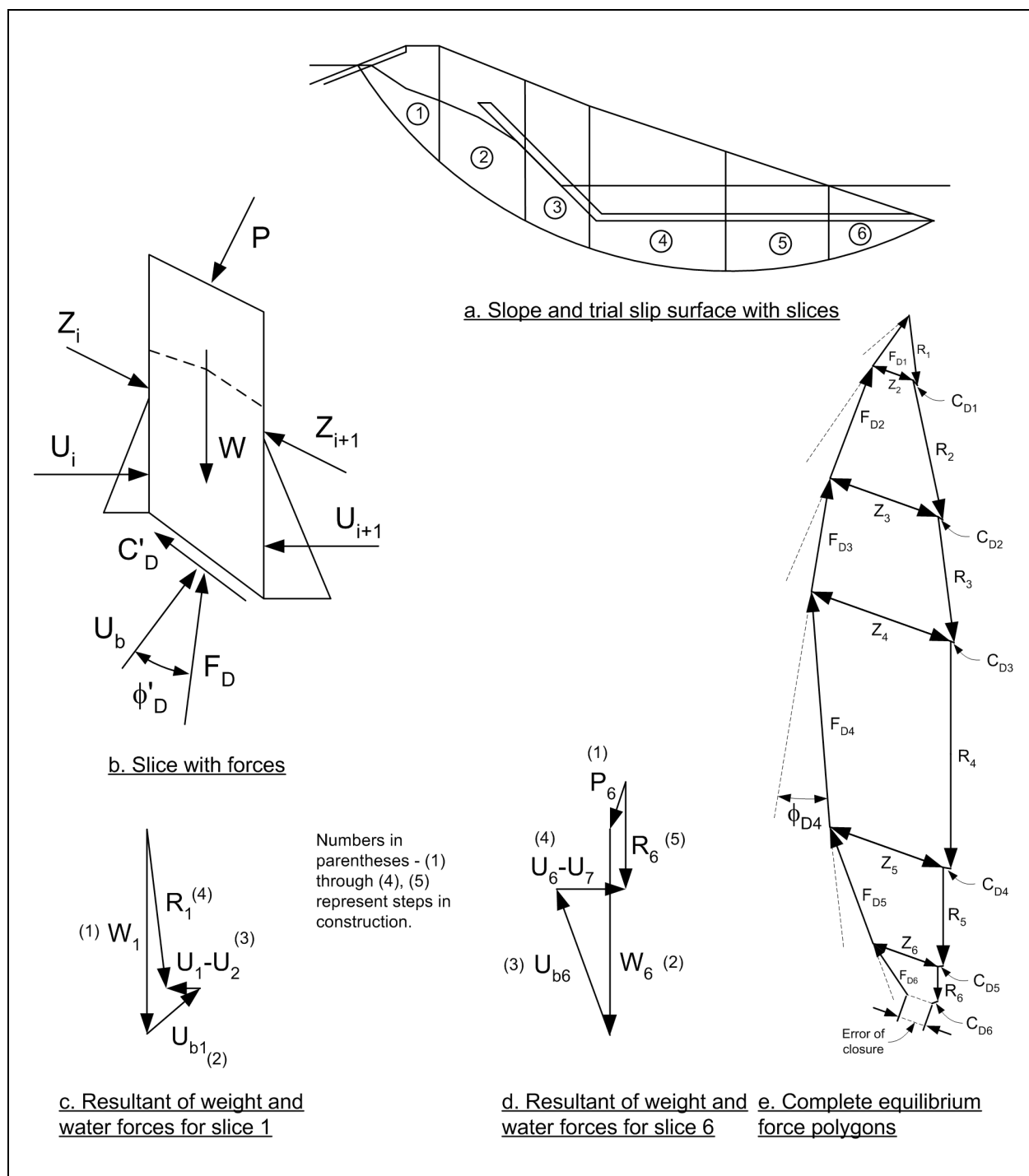


Figure F-9. Modified Swedish Method – graphical solution with water – force polygons

Figure F-8b). The developed friction angle,  $\phi_D$ , is computed from the relationship,  $\phi_D = \arctan \left( \frac{\tan \phi'}{F_1} \right)$  (Column 24 in Figure 8b). The trial force equilibrium polygons can now be constructed as described in the following steps.

(9) The resultant force from the weight of the slice and any water pressures on the top, sides, and bottom of the slice are determined for each slice separately. The first step in determining this resultant involves drawing a vector representing the water load on the top of the slice, as shown for the last slice in Figure F-9d. This water force vector, and all subsequent vectors, are drawn to the same scale.

(10) The second step in determining the resultant is to draw a vector representing the weight of the slice vertically downward from the tip of the vector representing the water loads on the top of the slice drawn in Step 9. See Figures F-9c and F-9d, for the first and last slices. If there are no external water loads, the weight vector is drawn from any convenient starting point, as in Figure F-9c.

(11) A vector representing the force,  $U_b$ , resulting from water pressures on the bottom of the slice is drawn extending from the tip of the weight vector in a direction perpendicular to the base of the slice (See  $U_{b1}$  and  $U_{b6}$  in Figures F-9c and F-9d).

(12) A vector representing the difference between the forces from water pressures on the upslope and downslope sides of the slice,  $U_i - U_{i+1}$ , is drawn horizontally, starting at the tip of the vector drawn in Step 11 (See  $U_1 - U_2$  and  $U_6 - U_7$  in Figures F-9c and F-9d).

(13) A vector,  $R$ , is drawn from the start of the vector representing the water loads,  $P$ , on the top of the slice, to the tip of the vector that was drawn in Step 12 to represent the water loads on the sides of the slice (See vector  $R_6$  in Figure F-9d). If there is no water load on the top of the slice, the vector is drawn starting at the point where the weight vector,  $W$ , was started (Figure F-9c). The  $R$ -vector closes the force polygon for the known water and gravity forces (Figures F-9c and F-9d). The  $R$ -vector represents the resultant force produced by the slice weight and water pressures on the top, sides, and bottom of the slice. Steps 9 through 13 are carried out for each slice individually.

(14) The set of force polygons for the entire slope are begun by drawing a vector representing the force,  $R_1$ , for the first slice, beginning at a convenient starting point, as shown in Figure F-9e.

(15) A vector representing the developed cohesion force,  $C_{D1}$ , is drawn in a direction parallel to the base of the first slice, extending from the tip of the resultant force vector,  $R_1$ , drawn in Step 14.

(16) A line is drawn from the start (tail) of the resultant force vector ( $R_1$ ) in a direction perpendicular to the base of the slice. This line is shown as a broken line in Figure F-9e.

(17) A second line is drawn from the start (tail) of the resultant force vector ( $R_1$ ) such that the new line makes an angle equal to the developed friction angle,  $\phi_D$ , with the vector drawn in Step 16. The new line should be drawn so that the component of the vector parallel to the bottom of the slice (the shear component) acts in the direction of the resisting shear force, i.e., counter-clockwise from the normal vector in the case of a right-facing slope like the one shown in Figure F-9. This vector is labeled  $F_{D1}$  in Figure F-9e.

(18) A line is drawn from the tip (end) of the developed cohesion vector, in the direction assumed for the interslice forces. This line is labeled  $Z_2$  in Figure F-9e. If hand calculations are being performed to check computations that were performed with Spencer's Method, the side force inclination should be the one found with Spencer's Method. Otherwise, the side force inclination should be assumed in accordance with the guidelines and discussion presented in Appendix C.

(19) The intersection between the two line directions drawn in Steps 17 and 18 is found. This determines the magnitude of the forces  $F_{D1}$  and  $Z_2$ .

(20) The process described above in Steps 14 through 19 is continued for the next slice, where a vector representing the resultant force,  $R_2$ , for the second slice is drawn from the point where the developed cohesion vector,  $C_{D1}$ , and interslice vector,  $Z_2$ , intersect. The force polygon for the second slice is shown in Figure F-9e. Closure of the force polygon is used to determine the magnitude of the forces  $F_{D2}$  and  $Z_3$  for the second slice.

(21) Force polygons are drawn slice-by-slice for the remaining slices. If the trial value of factor of safety is not the correct value, the force polygon for the last slice will not close. This error of closure is a measure of the inaccuracy in the assumed value for the factor of safety. Additional trial values are assumed for the factor of safety until the equilibrium force polygons close with an acceptable degree of accuracy. By plotting the error of closure versus the assumed values of factor of safety as shown in Figure F-6c, the correct value of factor of safety can usually be determined within a few trials.

## F-5. End-of-Construction (Short-Term Stability) Example

Example calculations are presented for stability at the end of construction of the embankment shown in Figure F-10. The embankment cross section contains two materials -- the embankment soil and the foundation soil. Both soils are fine-grained and undrained during construction.

*a. Shear Strengths.* Because the soils in this case are do not drain during construction, undrained shear strengths are used for both. For the embankment, samples would be prepared by compacting representative samples of the fill material at appropriate densities and moisture contents. For the natural foundation soil, undisturbed samples would be obtained for testing. The shear strengths would be determined using Unconsolidated-Undrained (UU or Q) triaxial compression tests. If the natural soil was saturated, Consolidated-Undrained (CU or R) or field vane shear tests could also be used to estimate undrained shear strengths, as described in Appendix D.

(1) Compacted, fined-grained fills are always partly saturated at the end of construction. The foundation soil in this example is also assumed to be partly saturated. Thus, the shear strengths of both soils are characterized by total stress friction angles greater than zero. If the foundation soil was saturated, its total stress friction angle,  $\phi$ , would be equal to zero.

(2) If the embankment contained zones of free-draining soils, their strengths would be characterized using effective stress shear strength parameters.

*b. Water pressures.* For the example problem illustrated in Figure F-10, all water pressures are zero, because there is no external water. If external water exists, the external water loads would be computed and included in the analysis in the same way they are included in the example described previously where there was water outside the slope. External water loads must always be included, regardless of whether the shear strength is represented using total or effective stresses. Because the strengths are characterized in terms of total stresses, pore water pressures within the slope are not included. However, if the embankment contained free-draining soils being characterized in terms of effective stress, pore water pressures would be included in the analysis for these materials.

*c. Unit weights.* Total unit weights are used for all soils. Total unit weights should always be used, regardless of whether the shear strength is represented using total or effective stresses. The total unit weights for the example problem are shown in Figure F-10b.

*d. Simplified Bishop Method.* Calculations using the Simplified Bishop Method for the example are illustrated in Figure F-11. Slices 6 through 10 contain both embankment and foundation soils, and these slices were divided into two portions for calculating the slice weights. The average height in each soil was

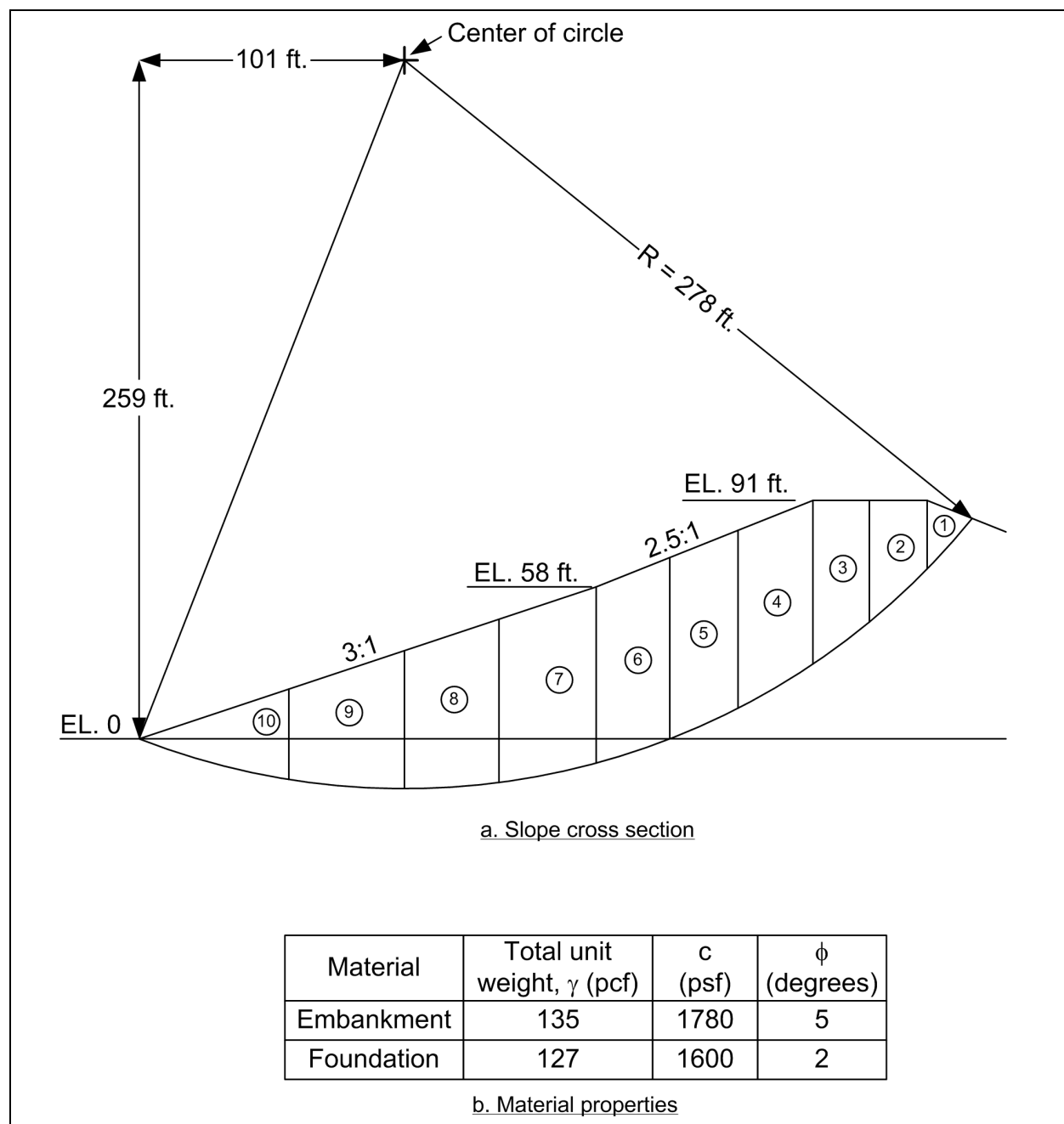


**Figure F-10. Slope used for example calculations for end-of-construction stability condition**

determined and used to compute the area and weight for that portion of the slice. The weights of two parts of the slices were then added to compute the total slice weight. The bottoms of slices 1 through 5 are located in the embankment soil and were assigned the shear strength properties of the embankment. The bottoms of slices 6 through 10 are located in the foundation, and these slices were assigned the shear strength properties of the foundation soil. Computations for the final value of the factor of safety ( $F = 1.33$ ) are shown in Columns 14 and 15 of the table in Figure F-11. Computations were also performed for three trial values for the factor of safety: 1.0, 1.5, and 2.0. The computed values for each trial value are plotted versus the assumed values in Figure F-11d. As can be seen in this figure, the computed value of  $F$  varied only slightly with changes in the assumed value.

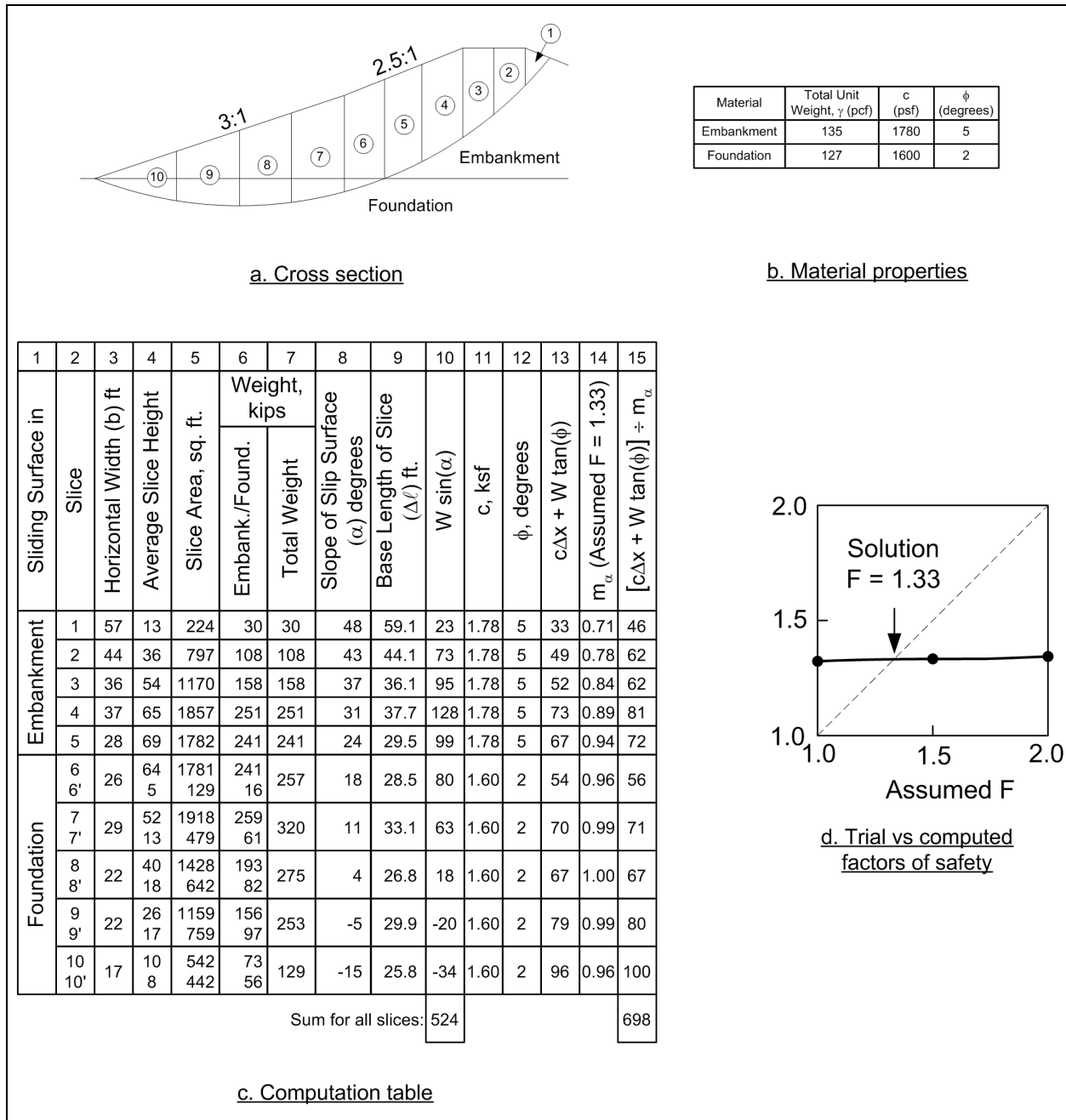


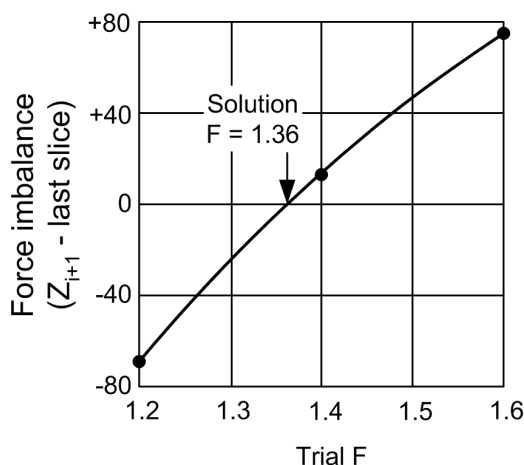
Figure F-11. End-of-construction example – Simplified Bishop Method

*e. Modified Swedish Method – numerical solution.* Calculations using numerical calculations for the Modified Swedish Method for the same slope are summarized in Figure F-12. For this example the interslice force inclination was assumed to be equal to the average embankment slope. The average embankment slope is 2.8 (horizontal) to 1 (vertical). The side force inclination used in the calculations was  $\theta = \arctan(1/2.8) = 19.7$  degrees.

1	2	3	4	5	6	7	8	9	10	11	12	13
Sliding Surface in	Slice	Horizontal Width (b) ft	Average Slice Height	Slice Area, sq. ft.	Weight, kips		Slope of Slip Surface ( $\alpha$ ) degrees	Base Length of Slice ( $\Delta L$ ) ft.	c, ksf	$\phi$ , degrees	$Z_i$ - Trial F = 1.6	$Z_{i+1}$ - Trial F = 1.6
					Embank./Found.	Total Weight						
Embankment	1	57	13	224	30	30	48	59.1	1.78	5	0	-8
	2	44	36	797	108	108	43	44.1	1.78	5	0	37
	3	36	54	1170	158	158	37	36.1	1.78	5	37	97
	4	37	65	1857	251	251	31	37.7	1.78	5	97	177
	5	28	69	1782	241	241	24	29.5	1.78	5	177	232
Foundation	6 6'	26	64 5	1781 129	241 16	257	18	28.5	1.60	2	232	277
	7 7'	29	52 13	1918 479	259 61	320	11	33.1	1.60	2	277	296
	8 8'	22	40 18	1428 642	193 82	275	4	26.8	1.60	2	296	270
	9 9'	22	26 17	1159 759	156 97	253	-5	29.9	1.60	2	270	193
	10 10'	17	10 8	542 442	73 56	129	-15	25.8	1.60	2	193	75

Negative interslice force set to zero for next slice.

a. Table used to compute factor of safety



b. Variation in force imbalance with trial factor of safety

Figure F-12. Example calculations for end-of-construction stability condition – Modified Swedish Method – numerical solution

(1) Many of the quantities shown in the table in Figure F-12a are the same as those for the Simplified Bishop Method in Figure F-11c. Only the interslice forces  $Z_i$  and  $Z_{i+1}$ , in Columns 12 and 13 in Figure F-12a, are different from the Simplified Bishop Method. The interslice forces were calculated by first assuming a trial value for the factor of safety, and setting  $Z_1$  for the first slice to zero. The value of  $Z_2$  was then calculated from Equation F-7. Values of the interslice forces were calculated successively for the remaining slices using

Equation F-7. Calculations are shown in the table in Figure F-12a for an assumed value of factor of safety equal to 1.6. The value of  $Z_{i+1}$  on the last slice is 75 kips, which represents the force imbalance, or error of closure, for this assumed factor of safety.

(2) Calculations were performed for three assumed values of factor of safety:  $F = 1.20, 1.40$ , and  $1.60$ . The force imbalances for these three factors of safety are plotted versus factor of safety in Figure F-12b. It can be seen from this figure that the correct value satisfying force equilibrium with essentially zero imbalance is approximately 1.36.

*f. Modified Swedish Method – graphical solution.* Calculations for the end-of-construction example using the graphical solution for the Modified Swedish Method are illustrated in Figures F-13 and F-14. The necessary numerical computations are shown in Figure F-13a. Most of the calculations and values shown in this table are the same as those shown previously for the numerical solution in Figure F-12. In addition, values for the force because of the developed cohesion,  $C_D$ , and the developed friction angle,  $\phi_D$ , are shown in Columns 12 and 13 of Figure F-13a. These values are shown for only one of the assumed values for the factor of safety ( $F = 1.6$ ). Three trial values (1.2, 1.4 and 1.6) were assumed for the factor of safety, and similar computations were made for each assumed value. The error of closure ( $Z_{i+1}$  for the last slice) is plotted versus the assumed value of factor of safety in Figure F-13b. The equilibrium force polygons are shown in Figure F-14 for a trial value for the factor of safety of 1.6. For this assumed value the error of closure is 75 kips. Note that the force polygons for the first three slices are shown twice in Figure F-14 to the same force scale as for the other slices, and to an expanded scale for clearer illustration.

## F-6. Steady Seepage (Long-Term Stability) Example

Figure F-15 shows an embankment with steady seepage. The cross section contains two principal zones -- the embankment fill and the foundation. There are also three smaller zones of material in the embankment: an upstream layer of rip-rap, an internal chimney drain and a horizontal drainage blanket. For these example stability calculations, all of these smaller zones were treated as being the same as the embankment. The trial slip surface used for the computations does not intersect any of the smaller zones, and their strength properties therefore do not influence the results of the analyses.

*a. Shear strengths.* For steady-state seepage conditions, drained shear strengths characterized by  $c'$  and  $\phi'$  are appropriate for all soils. The effective stress shear strength parameters are determined using consolidated-drained (CD or S) test procedures for testing coarse-grained soils, and consolidated-undrained (CU or R) test procedures with pore water measurements for fine-grained soils. The shear strength parameters used in this example are shown in the table at the top of Figure F-15. Samples of the embankment materials would be prepared by compacting samples at appropriate densities and moisture contents. For the natural foundation soils, test specimens would be obtained by undisturbed sampling.

*b. Water pressures.* The pore water pressures for the steady seepage condition were characterized by the piezometric line shown in Figure F-15. The piezometric line begins at the reservoir surface at the point where the reservoir intersects the fine-grained embankment soil (beneath the rip-rap), slopes downward to intersect the inclined chimney drain, then follows along the bottom side of the chimney drain until it reaches the elevation of the tailwater (el 22.5) and, finally, extends horizontally to the downstream face of the slope at the tailwater level. Pore water pressures are calculated for each slice by multiplying the vertical distance between the center of the base of the slice and the piezometric line by the unit weight of water. Alternatively, a more rigorous seepage analysis could have been performed and the pore water pressure from this analysis used in the computations. For the slip surface and slices illustrated in Figure F-16 there is only water on the external surface of the slope above the last slice, Slice 9. The external water load on the last slice is calculated and included in the computations for the factor of safety.

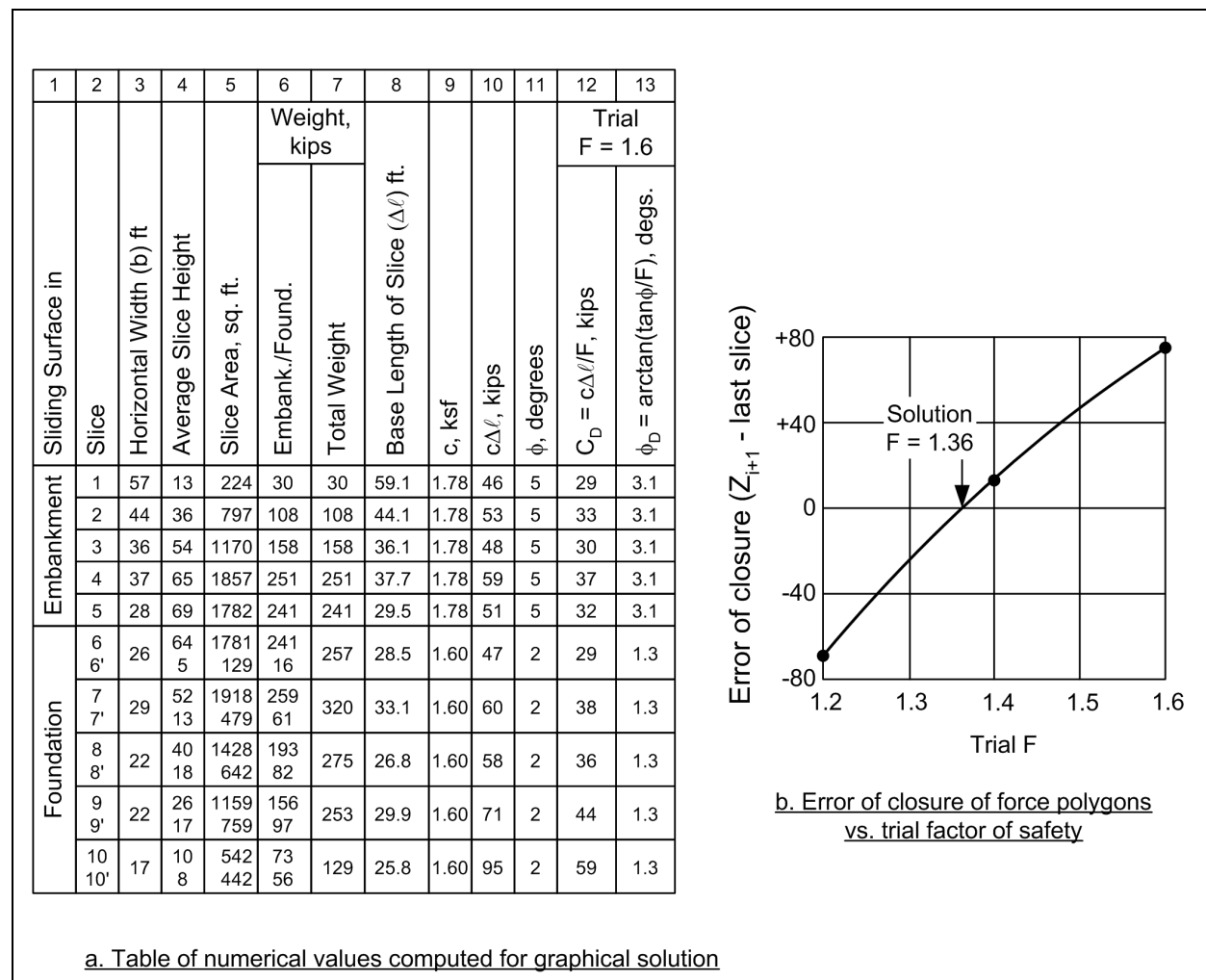


**Figure F-13. Example calculations for end of construction stability condition – Modified Swedish Method – numerical computations for graphical solution**

c. *Unit weights.* Total unit weights are used for all soils. Total unit weights should always be used regardless of whether the shear strength is represented using total or effective stresses. The total unit weights for the example problem are shown in the table at the top of Figure F-15.

d. *Slip surface and slices.* The circular slip surface shown in Figure F-16 was used for the example stability calculations. This surface is not the most critical slip surface. The factor of safety for an infinite slope failure in the upper part of the slope ( $F = 1.68$ ) is lower than the factor of safety ( $F = 2.01$ ) for the slip surface shown in Figure F-16. The infinite slope slip surface is very shallow, however, and the factor of safety for that failure mechanism is of less significance with respect to the safety of the embankment than the slip surface shown in Figure F-16. The soil above the slip surface is divided into the nine slices shown in Figure F-16. The same circle and slices are used for both the Simplified Bishop and the Modified Swedish Method analyses.

e. *Simplified Bishop Method.* Calculations performed using the Simplified Bishop Method are shown in Figure F-17. Slices 4 through 9 contain both embankment and foundation soil and were divided into two sections to calculate the slice weight. The average height in each soil was determined and used to compute the area and weight for that portion of the slice. The weights of two parts of the slices were then added to



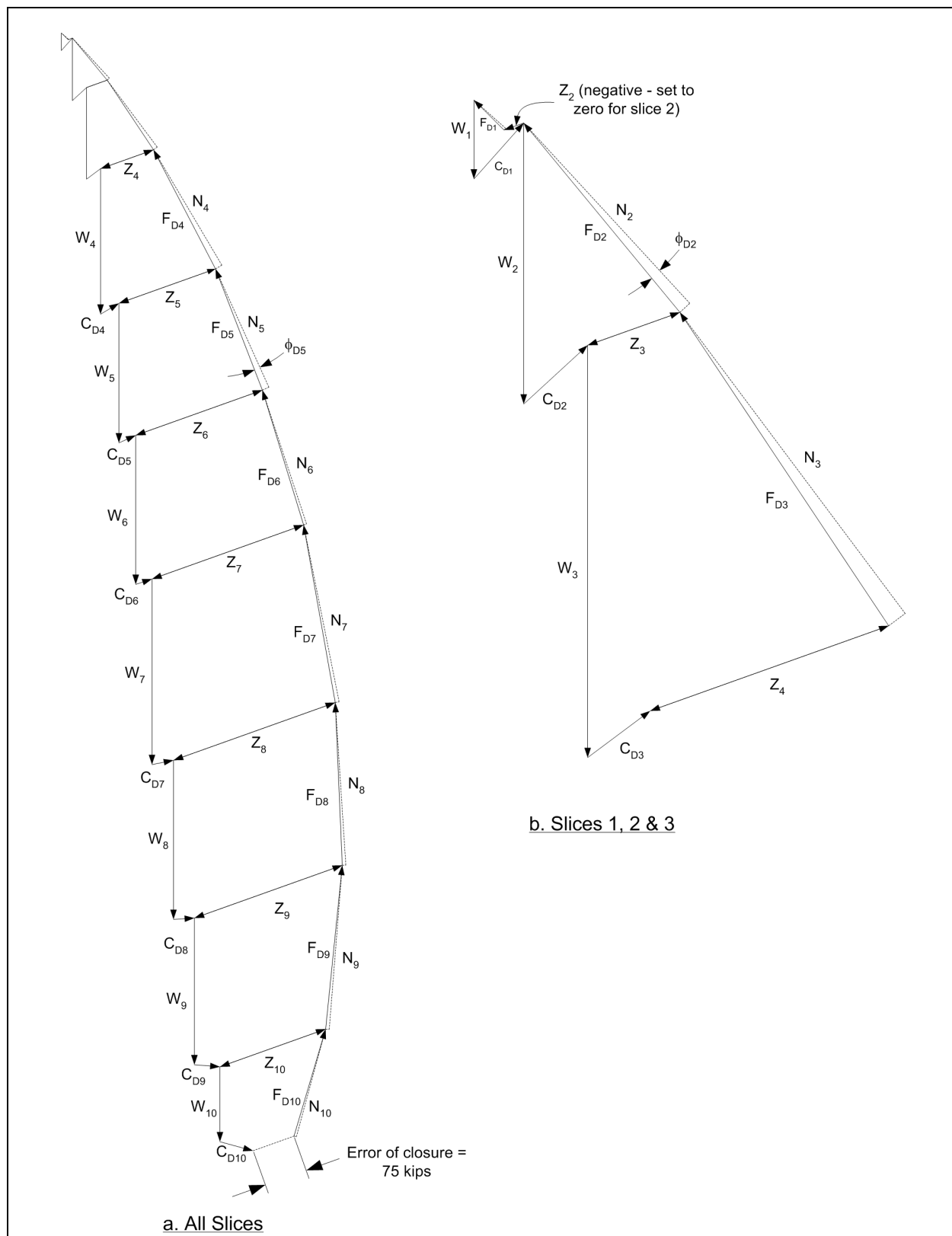


Figure F-14. Example calculations for end of construction stability condition – Modified Swedish Method – force polygons for graphical solution

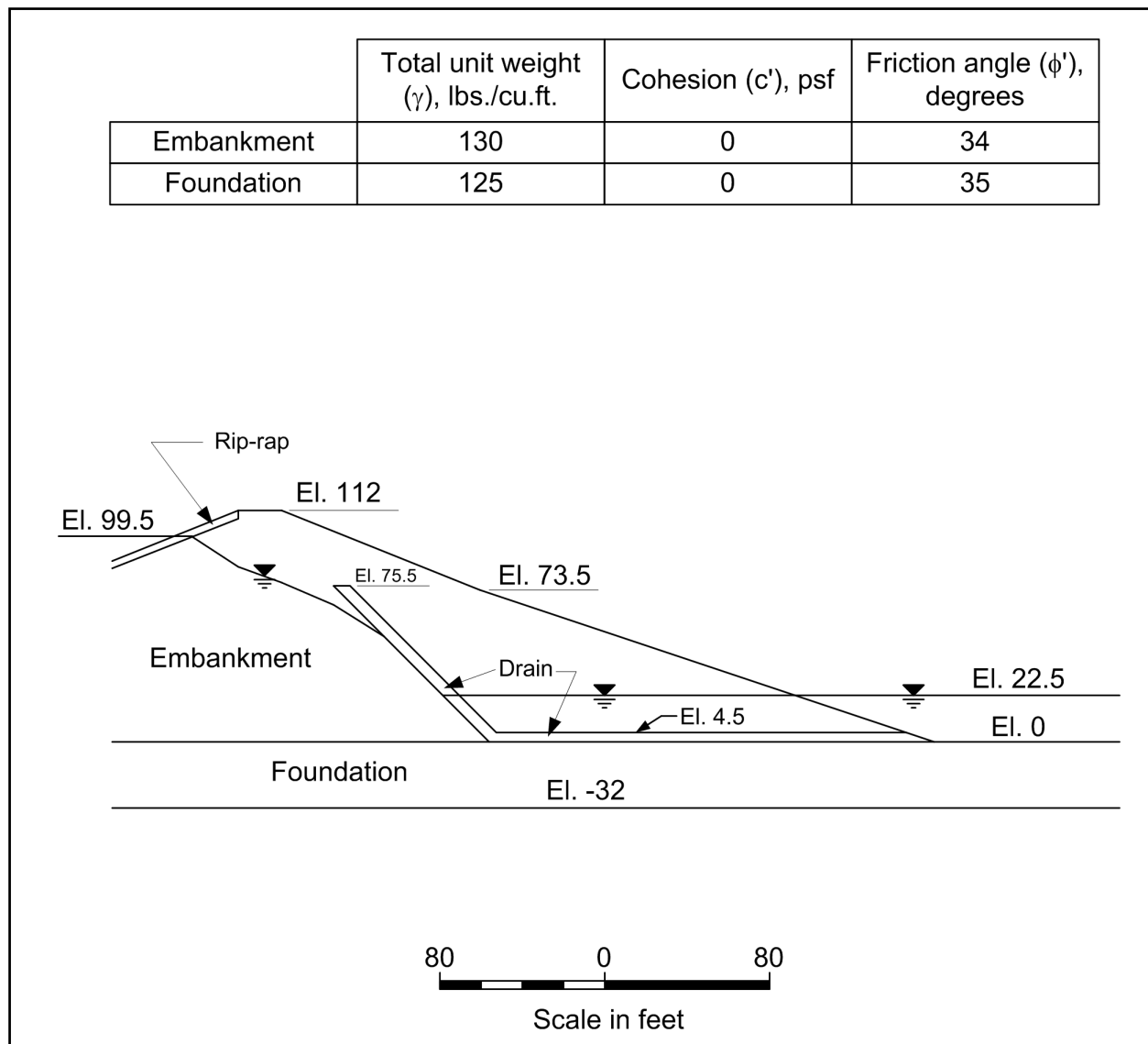
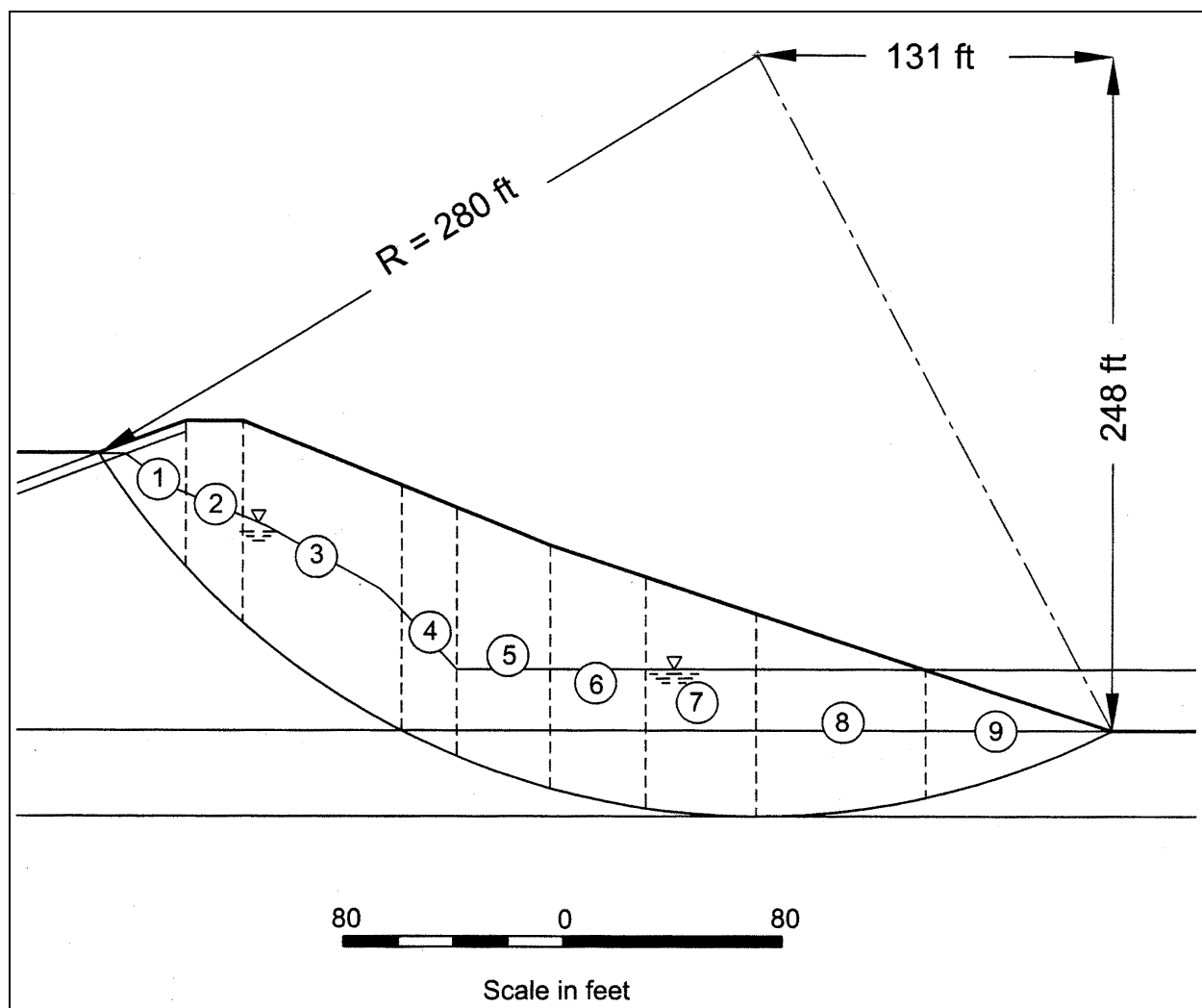


Figure F-15. Slope for example steady seepage computations

compute the total slice weight. The bottoms of Slices 1 through 3 are located in the embankment and these slices were assigned the shear strength properties of the embankment soil ( $c' = 0$ ,  $\phi' = 34$  degrees). The bottoms of slices 4 through 9 are located in the foundation soil and these slices were assigned the shear strength properties of the foundation ( $c' = 0$ ,  $\phi' = 35$  degrees). Computations are shown in Columns 22 and 23 of the table in Figure F-17a for the final value of the factor of safety ( $F = 2.01$ ). Computations were also performed for trial values of the factor of safety of 1.5, 2.0, and 2.5. The computed values are plotted versus the assumed values in Figure F-17b. The calculated values varied only slightly with the assumed value, as shown in Figure F-17b.

*f. Modified Swedish Method – numerical solution.* Calculations using the numerical solution for the Modified Swedish Method are summarized in Figure F-18. For this example the interslice force inclination was assumed to be equal to the average embankment slope. The average embankment slope is 2.8 (horizontal) to 1 (vertical). The side force inclination used in the calculations was  $\theta = \arctan (1/2.8) = 19.7$  degrees. Except for the forces from water pressures, most of the calculations and quantities shown in



**Figure F-16. Circular slip surface and slices used for example computations for steady-state seepage**

the table in Figure F-18 are the same as the ones used previously for the Simplified Bishop Method. The interslice forces,  $Z$ , are considered to be the effective forces and the water pressures on the sides of the slices are calculated independently. The calculations for the water pressures on the sides and top of the slices are shown in Columns 8 through 17 in the table in Figure F-18a. Calculation of the interslice forces is summarized in Column 23 in Figure F-18a for the final value of the factor of safety ( $F = 2.07$ ), which satisfies force equilibrium. Calculations were also performed for three trial values of factor of safety  $F = 1.75, 2.00$ , and  $2.25$ . The force imbalance for each assumed value of factor of safety is plotted versus the factor of safety in Figure F-18b. It can be seen that a value of  $F$  of  $2.07$  results in zero force imbalance.

*g. Modified Swedish Method – graphical solution.* Calculations using the graphical solution for the Modified Swedish Method are shown in Figures F-19, F-20, and F-21. The necessary numerical computations and the variation in error of closure with the assumed factor of safety are shown in Figure F-19. The force vector diagrams for the resultants of the forces due to water pressures and the weight of the slice ( $R_1, R_2$ , etc) are shown in Figure F-20. Finally, the equilibrium force polygons are shown in Figure F-21 for the final solution ( $F = 2.07$ ), where the force polygons close without significant force imbalance.

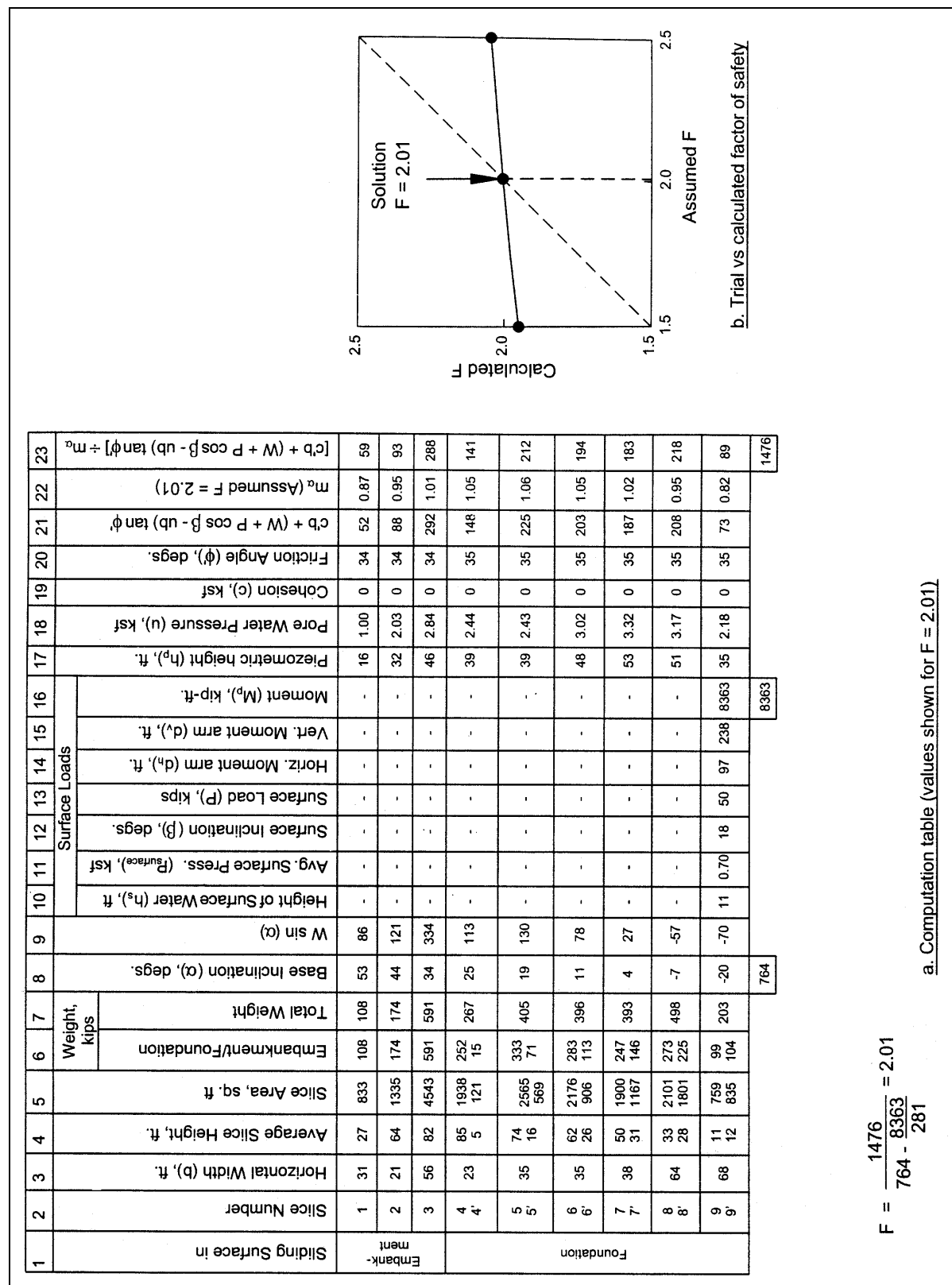


Figure F-17. Sample calculations for steady-state seepage – Simplified Bishop Method



a. Table of numerical values computed for graphical solution

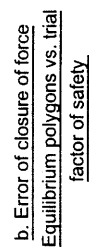


Figure F-19. Sample calculations for steady-state seepage – Modified Swedish Method – graphical solution - numerical values

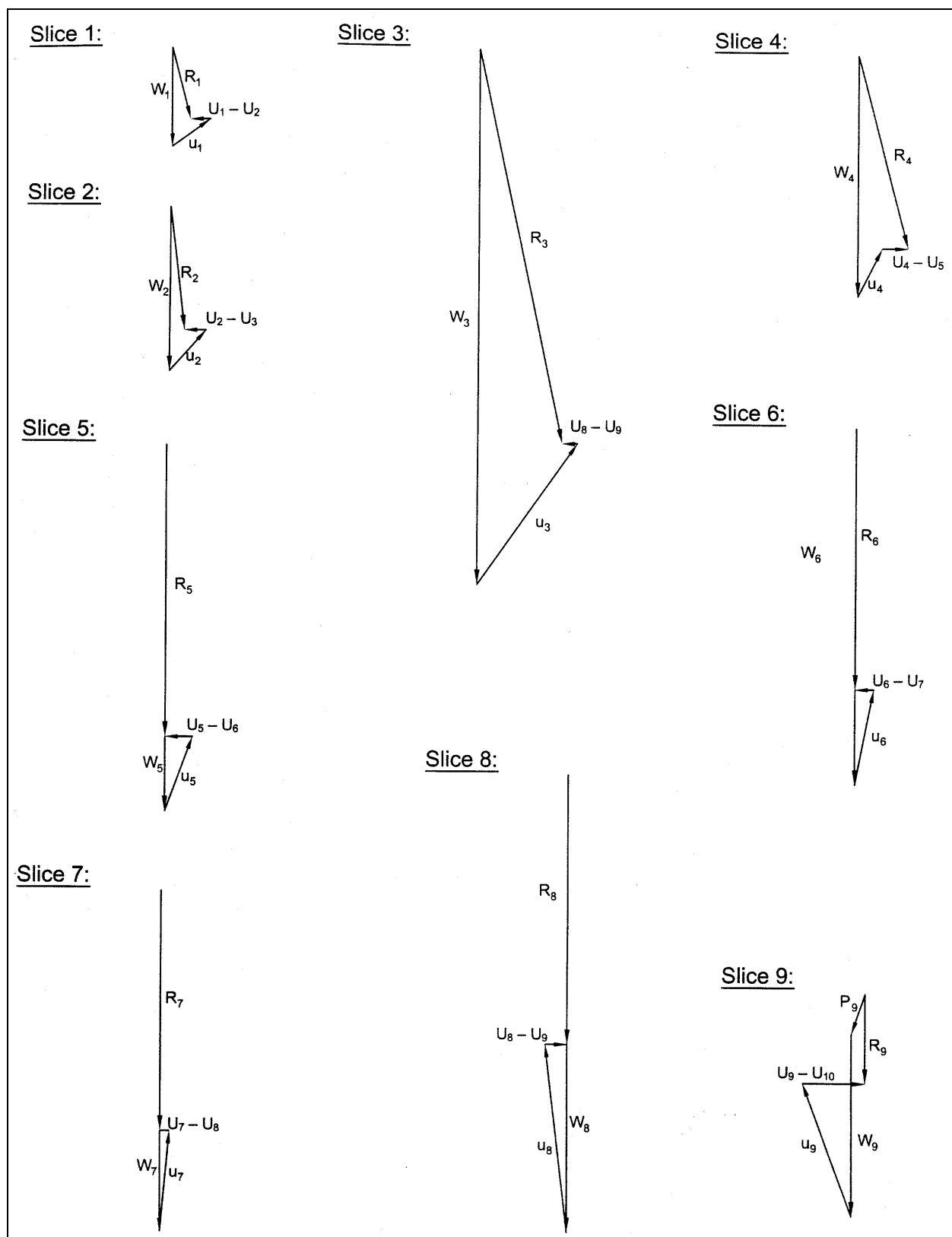


Figure F-20. Sample calculations for steady-state seepage – Modified Swedish Method – graphical solution – resultant force (R) diagrams

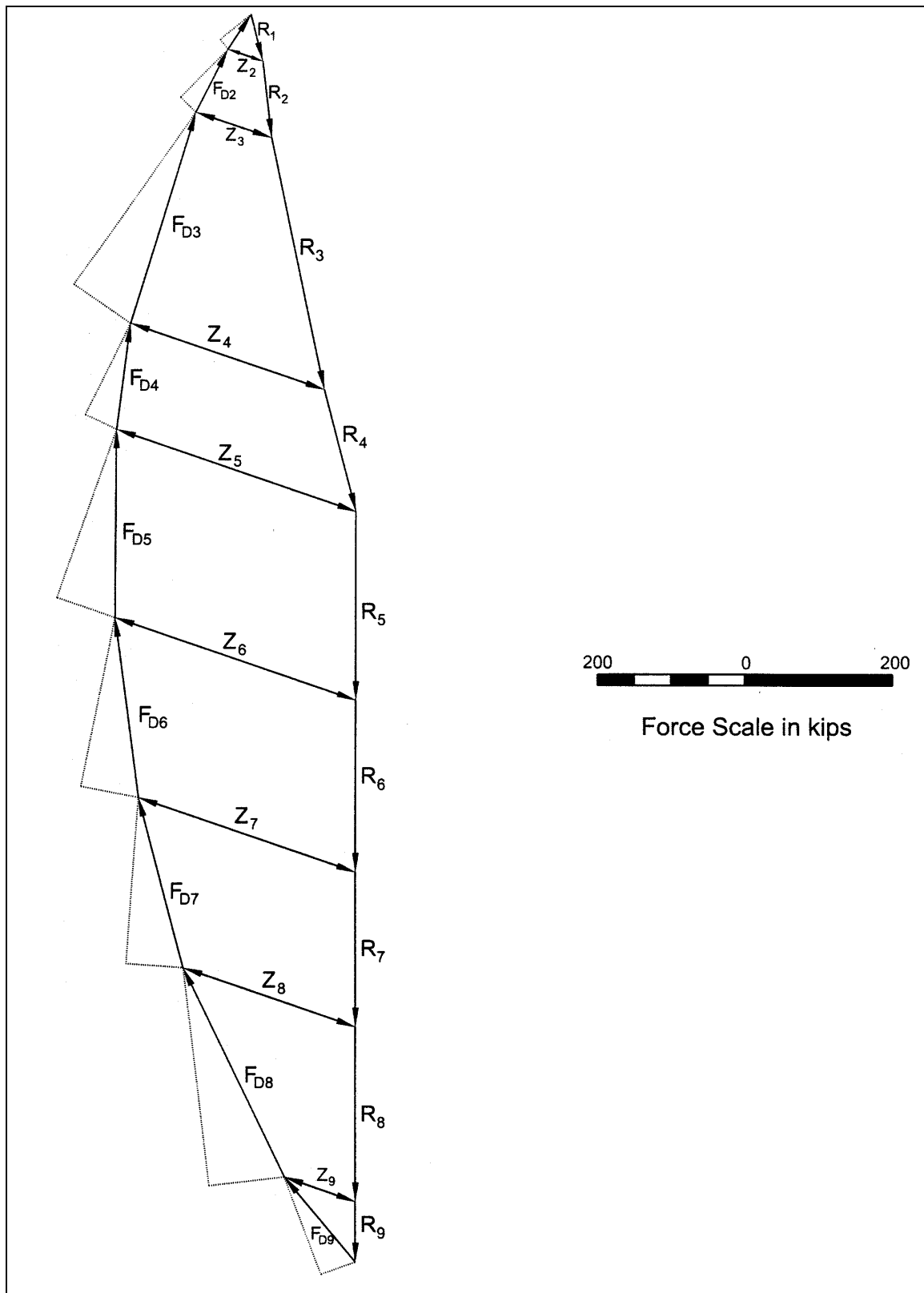


Figure F-21. Sample calculations for steady-state seepage – Modified Swedish Method – graphical solution – force equilibrium polygons